# FINAL REPORT

## Hexachloroethane Obscurant Replacement

SERDP Project WP-2149

JANUARY 2012

Reed Blau
Nathan Seidner
**ATK Launch Systems Inc.**



SERDP
DOD ▪ EPA ▪ DOE

# REPORT DOCUMENTATION PAGE

*Form Approved*
*OMB No. 0704-0188*



| **1. REPORT DATE** *(DD-MM-YYYY)* | **2. REPORT TYPE** | **3. DATES COVERED** *(From - To)* |
|---|---|---|
| 02-04-2012 | Final Report | June 2011-March 2012 |

**4. TITLE AND SUBTITLE**
Hexachloroethane Obscurant Replacement

**5a. CONTRACT NUMBER**
W912HQ-11-C-0002

**5b. GRANT NUMBER**

**5c. PROGRAM ELEMENT NUMBER**

**6. AUTHOR(S)**
Reed Blau
Nathan Seidner

**5d. PROJECT NUMBER**

**5e. TASK NUMBER**

**5f. WORK UNIT NUMBER**

**7. PERFORMING ORGANIZATION NAME(S) AND ADDRESS(ES)**

ATK Propulsion Systems
P.O. Box 707 Brigham City, UT 84302

**8. PERFORMING ORGANIZATION REPORT NUMBER**
TR031214

**9. SPONSORING / MONITORING AGENCY NAME(S) AND ADDRESS(ES)**

Strategic Environmental Research and Development Program

901 N. Stuart Street, Suite 303 Arlington, VA 22203

**10. SPONSOR/MONITOR'S ACRONYM(S)**
SERDP

**11. SPONSOR/MONITOR'S REPORT NUMBER(S)**

**12. DISTRIBUTION / AVAILABILITY STATEMENT**
Document cleared for public release; distribution unlimited

**13. SUPPLEMENTARY NOTES**

**14. ABSTRACT** A variety of pyrotechnic compositions were investigated for their viability as replacements for hexachloroethane based obscurants. The investigations included combustion modeling, ingredient and composition thermal compatibility and sensitivity to significant impact, friction and electrostatic discharge events. Candidates were screened through the combustion of small samples {less than ten grams} via open burning and combustion in a 100 cubic foot chamber to determine smoke density and analyze for toxicity of combustion gases and particulates. Compositions containing boron potassium nitrate igniter blended with halide salts {cesium, potassium and ammonium} were studied in greatest detail. Solids produced from the combustion of the specific compositions selected for study were not totally dispersed in aerosol form; significant solid slag formation was observed. Thus, smoke density efficiency was only one quarter of that of the hexachloroethane containing baseline. The addition of lower levels of the halide salt coolant to the boron potassium nitrate igniter may improve overall obscurant efficiency. Although the specific formulations tested did not perform as well as the hexachloroethane baseline, formulation variants were identified which should have improved performance.

**15. SUBJECT TERMS**
Non-toxic obscurant, hexachloroethane smoke replacement

| **16. SECURITY CLASSIFICATION OF:** | | | **17. LIMITATION OF ABSTRACT** | **18. NUMBER OF PAGES** | **19a. NAME OF RESPONSIBLE PERSON** |
|---|---|---|---|---|---|
| **a. REPORT** | **b. ABSTRACT** | **c. THIS PAGE** | | | Nathan Seidner |
| U | U | U | U | 57 | **19b. TELEPHONE NUMBER** *(include area code)* (435) 863-4486 |

**Standard Form 298 (Rev. 8-98)**
**Prescribed by ANSI Std. Z39.18**

## ABSTRACT

**Objective:** When the AN-M8 handheld smoke grenade is functioned, it produces a hexachloroethane based {HCE} smoke. This smoke can cause a number of medical problems that range from cough and difficulty breathing to chemical pneumonitis, pulmonary edema, adult respiratory distress syndrome, severe liver problems and death. These health issues pose a threat to the health of the war fighters that are exposed to this smoke during training and combat. The objective of the proposed work is to demonstrate a pyrotechnic formulation at a lab scale that can match or exceed the opacity, duration of obscuration and area of coverage of the smoke produced by an AN-M8 handheld grenade.

**Technical Approach:** A variety of pyrotechnic compositions were investigated for their viability as replacements for hexachloroethane based obscurants. The investigations included combustion modeling, ingredient and composition thermal compatibility and sensitivity to significant impact, friction and electrostatic discharge events. Candidates were screened through the combustion of small samples {less than ten grams} via open burning and combustion in a 100 cubic foot chamber to determine smoke density and analyze for toxicity of combustion gases and particulates.

**Results:** Compositions containing divalent zinc and copper oxidizers combined with ammonium chloride were deemed to be thermally incompatible. Compositions containing sodium nitrate, silicon powder and polydimethylsilicone binder improved in performance as the ratio of silicon powder to silicone polymer decreased and the total fuel content increased.

Compositions containing boron potassium nitrate igniter blended with halide salts {cesium, potassium and ammonium} were studied in greatest detail. Solids produced from the combustion of the specific compositions selected for study were not totally dispersed in aerosol form; significant solid slag formation was observed. Thus, smoke density efficiency was only one quarter of that of the hexachloroethane containing baseline. The addition of lower levels of the halide salt coolant to the boron potassium nitrate igniter may improve overall obscurant efficiency. The overall toxicity of combustion gases and particulates is lower for boron potassium igniter blended with cesium or potassium chloride relative to the hexachloroethane baseline obscurant.

**Benefits:** Informative, reproducible methods were developed for characterization of the smoke density of particulate aerosols, and the determination of particulate concentrations, particulate particle size distributions as well as the chemical composition of the particles and toxic gases produced from baseline and candidate obscurants. Hazards for processing and testing the obscurants were well defined and controlled. Although the specific formulations tested did not perform as well as the hexachloroethane baseline, formulation variants were identified which should have improved performance.

**TABLE OF CONTENTS**

ABSTRACT ..... I

LIST OF FIGURES ..... IV

LIST OF TABLES ..... V

LIST OF SYMBOLS, ABBREVIATIONS AND ACRONYMS ..... VI

ACKNOWLEDGEMENTS ..... VII

1.0 PREFACE ..... 1

2.0 SUMMARY ..... 2

3.0 INTRODUCTION ..... 3

4.0 METHODS, ASSUMPTIONS AND PROCEDURES ..... 3
- 4.1 Thermochemical Modeling ..... 3
- 4.2 Preliminary Environmental and Human Health Assessment ..... 4
- 4.3 Compatibility Testing ..... 4
- 4.4 Speed Mixing ..... 5
- 4.5 Hazard Sensitivity Testing ..... 5
- 4.6 Pressing of Dry Blended Obscurant Samples ..... 8
- 4.7 Initial Obscurant Formulation Screening ..... 8
- 4.8 Obscurant Analysis in the 100 Cubic Foot Chamber ..... 9
- 4.9 Particulate and Toxic Gas Analysis at Autoliv Americas ..... 13
  - 4.9.1 Ignition ..... 13
  - 4.9.2 Gas Sampling and Analysis ..... 14
  - 4.9.3 Total Particulate Sampling and Analysis ..... 14
  - 4.9.4 Particulate Size Distribution Measurements ..... 14
  - 4.9.5 Chemical Analysis of Respirable Particulate ..... 15

5.0 RESULTS AND DISCUSSION ..... 16
- 5.1 Silicon Based Obscurant Candidates ..... 16
  - 5.1.1 Thermochemical Modeling ..... 16
  - 5.1.2 Ingredient Compatibilities ..... 17
  - 5.1.3 Hazard Sensitivity Data ..... 18
  - 5.1.4 Initial Formulation Screening ..... 23
  - 5.1.5 Hundred Cubic Foot Chamber Tests ..... 24
- 5.2 Boron/Potassium Nitrate Based Obscurant Candidates ..... 24
  - 5.2.1 Thermochemical Modeling ..... 25
  - 5.2.2 Ingredient Compatibilities ..... 29
  - 5.2.3 Hazard Sensitivity ..... 32
  - 5.2.4 Initial Formulation Screening ..... 32
  - 5.2.5 Pellet Density Measurements ..... 34
  - 5.2.6 Hundred Cubic Foot Chamber Transmittance Analysis at ATK ..... 34
  - 5.2.7 Hundred Cubic Foot Chamber Particulate Analysis at Autoliv ..... 36

5.2.8 Toxic Gas Analysis ..... 40
5.2.9 Chemical Analysis of Respirable Obscurant Particulates ..... 42
5.3 Divalent Metal Oxidizers with Ammonium Halide Fuels ..... 46
5.3.1 Thermochemical Modeling ..... 46
5.3.2 Ingredient Characterization: Metal Diborides as Fuels in Obscurant Formulations 48
5.3.3 Thermal compatibilities ..... 49

6.0 CONCLUSIONS ..... 54

7.0 RECOMMENDATIONS ..... 54

8.0 REFERENCES ..... 56

## LIST OF FIGURES

Figure 1: FlackTek SpeedMixer {left}, mixing cup {center}, SpeedMixer mixing compartment with mixing cup placed cup holder system {right} ..... 5
Figure 2: ABL Impact Machine ..... 5
Figure 3: ABL Friction Machine ..... 6
Figure 4: ABL ESD test apparatus {12}, close-up view of the ESD needle, stand and sample enclosure {right} ..... 7
Figure 5: Diagram of an SBAT cell ..... 7
Figure 6: Carver hand operated press: platen {left}, pressure gauges {top right}, hand operated pressure control system {bottom right} ..... 8
Figure 7: Test equipment used for initial obscurant formulation screening. Hood designated for ignition and combustion characterization of 0.05-5.0 grams of pyrotechnics {left}, variable output power supply {top right}, sample holder and ignition wand with tungsten ignition wire {bottom right} ..... 9
Figure 8: Obscurant 100 cubic foot test chamber {left}, light source for transmittance measurements {bottom right}, light detector, air inlet and gas sampling ports {top center}, pellet ignition system {top right} ..... 11
Figure 9: HCE obscurant replacement samples prepared for testing {left}, pellet ready for igntion {right} ..... 11
Figure 10: Representative voltage vs. time curves {voltage is proportional to transmittance} obtained from 100 cubic foot chamber tests on 3 gram pellets of HCE obscurant replacement formulations; 22Z, 22G and 22M; as well as corresponding traces for 3 grams {bottom left}, 2 grams {bottom middle} and 1 gram {bottom right} of HCE obscurant. .. 12
Figure 11: Gas monitoring devices: Draeger Tube Bellows {left}, Draeger CMS with ten chemical specific chips {center}, iBRID MX6 multi-gas monitor {right} ..... 13
Figure 12: Autoliv test equipment: 100 cubic foot chamber {left}, FT-IR {right} ..... 14
Figure 13: Andersen particulate particle size sampler ..... 15
Figure 14: DSC thermograms: sodium nitrate with Dow Corning silicone vacuum grease {green trace}; sodium nitrate with silicon powder {blue and red traces} ..... 19
Figure 15: DSC thermograms: sodium nitrate with RTV 615B {red trace}; RTV 615B alone {black trace}; sodium nitrate with RTV 615A {green trace}; RTV 615A alone {violet trace} ..... 20
Figure 16: DSC thermograms: silicon powder with RTV 615B {violet trace}; RTV 615B alone {green trace}; silicon powder with Dow Corning silicone vacuum grease {brown trace}; silicon powder with RTV 615A {blue trace}; RTV 615A alone {red trace} ..... 21
Figure 17: Test setup {left} and smoke output {right} of an IFBG containing an 18.2-gram net explosive weight shown two seconds after initiation of the grenade..... 25
Figure 18: DSC Thermograms for BKN {UIX-156}/KCl {black and violet traces} and BKN/CsCl {red and brown traces} ..... 30
Figure 19: DSC Thermograms for BKN/ACl {green and blue traces} and neat ACl {black trace} ..... 31
Figure 20: Comparison of HCE baseline transmittance with that of the BKN based obscurant candidates ..... 36
Figure 21: Average Anderson impactor data: top-all data, bottom-BKN formulations ..... 38
Figure 22: Hydrogen chloride levels plotted as a function of obscurant sample weight ..... 40

Figure 23: “Aged” VTS tubes containing $NH_4Cl$ {left}; 2-tubes of $NH_4Cl$/Cupric Oxide {center}; Cupric Oxide {right} ..... 50
Figure 24: DSC thermograms for ACl {black}, ACl/ZnO {blue} and ACl/B {red} ..... 51
Figure 25: DSC thermograms for ACl {black}, BCN {violet} and ACl/BCN {red} ..... 52
Figure 26: DSC thermograms for ACl {black}, Al/ACl {blue} and ACl/CuO {red} ..... 53

## LIST OF TABLES

Table 1: Toxic gases analyzed and method for their detection ..... 13
Table 2: Exemplary thermochemical calculations on potential HC smoke replacement formulations containing silicon. Formulations selected for experimentation are in bold ..... 17
Table 3: Summary of the VTS compatibility data for silicon based obscurant candidates ..... 22
Table 4: Hazard sensitivity data for silicon-based obscurant candidates ..... 23
Table 5: Thermochemical modeling of the BKN/KCl obscurant family ..... 26
Table 6: Thermochemical modeling of the BKN/CsCl obscurant family ..... 26
Table 7: BKN/KCl and BKN/CsCl formulations selected for performance evaluation ..... 27
Table 8: Thermochemical modeling of the BKN/$NH_4Cl$/KN obscurant family ..... 28
Table 9: BKN/ACl/KN formulations selected for performance evaluation ..... 29
Table 10: Compatibility data for HCE baseline ingredients and BKN with halide salts ..... 29
Table 11: Compatibility data for D50 Urethane adhesive with obscurant formulations ..... 29
Table 12: Hazard sensitivity data for the hexachloroethane baseline obscurant and the obscurant candidates containing BKN blended with halide salts ..... 33
Table 13: Comparison of obscurant pellet densities ..... 34
Table 14: Transmittance data ..... 35
Table 15: Autoliv total particulate data ..... 37
Table 16: Anderson impactor particulate values ..... 37
Table 17: Toxic gas analysis data ..... 41
Table 18: Additional toxic gases measured but not detected ..... 42
Table 19: Analysis of elements and ions in obscurant particulates ..... 43
Table 20: Upper possible concentration level of other elements or ions ..... 43
Table 21: Calculations for three-gram BKN/MCl tests in a 100 cubic foot chamber ..... 44
Table 22: Calculations for three-gram HCE Baseline tests in a 100 cubic foot chamber ..... 45
Table 23: Comparison of LD50 values for potassium and cesium salts ..... 46
Table 24: Combustion modeling data for divalent metal oxidizers with ammonium halides ..... 47
Table 25: Hazard sensitivity of aluminum and magnesium diborides ..... 49
Table 26: Thermal compatibility data for divalent metal oxidizers with ammonium chloride and boron. ..... 50

## LIST OF SYMBOLS, ABBREVIATIONS AND ACRONYMS

ABL.....Allegheny Ballistics Laboratory
ACFM .....actual cubic feet per minute
ACIGH.....American Conference of Industrial Hygienists
ACl.....ammonium chloride
AHOPs .....ATK Hazardous Operations Standard
ASTM .....American Society for Testing and Materials
ATK .....Alliant Techsystems Inc.
BCN .....basic copper nitrate, $Cu_2\{OH\}_2NO_3$
BKN .....boron potassium nitrate igniter
BKN/ACl .....blend of boron potassium nitrate igniter with ammonium chloride
BKN/CsCl.....blend of boron potassium nitrate igniter with cesium chloride
BKN/KCl .....blend of boron potassium nitrate igniter with potassium chloride
CMS .....chip measurement system
CsCl.....cesium chloride
CuO.....cupric oxide
$Cu_2\{OH\}_2NO_3$ .....basic copper nitrate
DSC.....differential scanning calorimetry
ESD.....electrostatic discharge
FT-IR.....Fourier transform-infrared spectroscopy
HCE.....hexachloroethane
IFBG .....Improved Flash Bang Grenade
IC.....ion chromatography
ICP AES.....inductively coupled plasma atomic emission spectrometry
KCl.....potassium chloride
KN.....potassium nitrate
LD50 .....median lethal dose
MCl .....metal chloride
mW.....milliWatts
NASA.....National Aeronautic and Space Administration
$NH_4Cl$.....ammonium chloride
NSWC.....Naval Surface Weapons Center
OSHA.....Occupational Safety and Health Administration
PBW.....percent by weight
PEL .....permissible exposure level
PSI.....pounds per square inch
SBAT .....simulated bulk autoignition temperature
SEED.....SERDP Exploratory Development Program
SERDP .....Strategic Environmental Research and Development Program
STEL .....short term exposure limit
TIL .....threshold initiation value
VAC .....volts alternating current
VTS .....vacuum thermal stability
WS.....water soluble
WIAS .....water insoluble, acid insoluble
WIAI .....water insoluble, acid insoluble
ZnO .....zinc oxide

## ACKNOWLEDGEMENTS

The author acknowledges the assistance of Brad Cragun and Bill Sampson during the initial formulation screening efforts, Rick Tanner for assistance in setting up the 100 cubic foot test chamber and developing obscurant test methods, Mai Nield for documenting the 100 cubic foot test chamber test method, Boyd Hill for conducting a hazards analysis for obscurant testing in the 100 cubic foot test chamber, Matt Brown for assistance in obscurant testing and data collection and Chris Peterson for supervising particulate and toxic gas characterization efforts at Autoliv Americas.

The Strategic Environmental Research and Development Program is gratefully acknowledged for their financial support of this research effort.

## 1.0 PREFACE

When the AN-M8 handheld smoke grenade is functioned, it produces a hexachloroethane based {HCE} smoke. This smoke can cause a number of medical problems that range from cough and difficulty breathing to chemical pneumonitis, pulmonary edema, adult respiratory distress syndrome, severe liver problems and death. These health issues pose a threat to the health of the war fighters that are exposed to this smoke during training and combat.

The objective of the proposed work is to demonstrate a pyrotechnic formulation at a lab scale that can match or exceed the opacity, duration of obscuration and area of coverage of the smoke produced by an AN-M8 handheld grenade. This data will allow for down selection of the best formulations and identify pertinent follow up work that will include scale up of refined formulations and their integration into prototype handheld smoke devices that can be used to replace the AN-M8.

## 2.0 SUMMARY

A variety of pyrotechnic compositions were investigated for their viability as replacements for hexachloroethane based obscurants. The investigations included combustion modeling, ingredient and composition thermal compatibility and sensitivity to significant impact, friction and electrostatic discharge events. Candidates were screened through the combustion of small samples {less than ten grams} via open burning and combustion in a 100 cubic foot chamber to determine smoke density and analyze for toxicity of combustion gases and particulates.

Combustion modeling was conducted on compositions containing divalent metal oxidizers, ammonium halides and a metallic fuel powder, either boron or aluminum. These compositions were predicted to produce significant quantities of deliquescent metal chloride combustion products. Boron combustion products also produce significant quantities of smoke. Compositions containing divalent zinc and copper oxidizers combined with ammonium chloride were deemed to be thermally incompatible. Similar compositions with calcium peroxide, calcium and zinc iodates show promise theoretically. Viability as obscurant compositions must be determined experimentally.

Compositions containing sodium nitrate, silicon powder and polydimethylsilicone binder improved in performance as the ratio of silicon powder to silicone polymer decreased and the total fuel content increased. For example, formulations with only 10% silicone grease produced primarily slag and little aerosol whereas formulations with 30% by weight cured RTV615 silicone produced little solid slag. Fuel rich formulations that required significant afterburning to complete combustion seemed to produce smoke most efficiently. Quantitative analysis of smoke density for the formulation family with cured silicone is warranted.

Compositions containing boron potassium nitrate igniter blended with halide salts {cesium, potassium and ammonium} were studied in greatest detail. Solids produced from the combustion of the specific compositions selected for study were not totally dispersed in aerosol form; significant solid slag formation was observed. Thus, smoke density efficiency was only one quarter of that of the hexachloroethane containing baseline. The addition of lower levels of the halide salt coolant to the boron potassium nitrate igniter may improve overall obscurant efficiency. This will occur by increasing the flame temperature of combustion allowing for more efficient volatilization of the solid combustion products. Burn rate will increase as coolant levels are decreased in the compositions.

The overall toxicity of combustion gases and particulates is lower relative to the baseline for at least the compositions where boron potassium nitrate igniter is blended with either potassium or cesium chloride. The baseline hexachloroethane obscurant produced high levels of hydrogen chloride and levels of zinc chloride and phosgene well above OSHA permissible exposure level limits. Formulations with boron potassium nitrate igniter and halide salts produced lower levels of hydrogen chloride, especially the composition containing cesium chloride. No OSHA permissible exposure limits are published for alkali halide particulate. No phosgene is produced upon their combustion although some nitrogen oxide is produced. The oxidizer/fuel balanced formulation containing ammonium chloride produced measurable levels of nitrogen dioxide also. Formulations of boron potassium nitrate with cesium chloride or potassium chloride should be pursued further especially at lower coolant levels. Of the formulations tested, those with cesium chloride were the most efficient candidates on a volumetric basis while producing the lowest level of toxic gases.

## 3.0 INTRODUCTION

The obscurant used in the AN-M8 handheld smoke grenade is hexachloroethane/zinc oxide combined with granular aluminum that burns to produce obscurant smoke. When ignited this pyrotechnic mixture releases several compounds including, zinc chloride, 62.5%; zinc oxide, 9.6%; iron oxide, 10.7%; aluminum oxide, 5.4%; lead oxide, 1%; and chlorinated vapors, 10.8% (1). The reaction that governs this reaction is as follows (2):

$$2\ Al + C_2Cl_6 + 3\ ZnO \rightarrow 3\ ZnCl_2 + Al_2O_3 + 2C + heat$$

The reaction is exothermic and creates large amounts of zinc chloride as a hot vapor. As the hot vapor cools, the zinc chloride nucleates to form a hygroscopic aerosol that rapidly absorbs water from the surrounding atmosphere. Hydrated zinc chloride particles then scatter light, thereby creating the desired obscurant effect (3); (4); (5). The heat released in this reaction causes other chemicals to form, including carbon tetrachloride, tetrachlorethylene, hexachlorobenzene, and phosgene (3).

Inhalation of HC smoke can cause a number of medical problems that range from cough and difficulty breathing to chemical pneumonitis, pulmonary edema, adult respiratory distress syndrome, severe liver problems and death (6); (7); (8); (9).

The focal point of this proposal is the use of pyrotechnics that produce obscuring smoke containing metal oxides as well as hygroscopic species such as sodium borate, sodium silicate, ammonium chloride, cesium chloride and potassium chloride. The presence of these hygroscopic species will help maximize the smoke output while avoiding the use of acidic smoke.

## 4.0 METHODS, ASSUMPTIONS AND PROCEDURES

### 4.1 Thermochemical Modeling

Thermochemical modeling was accomplished with the NASA Lewis Thermochemical code to help optimize smoke output and minimize undesirable species such as hydrochloric acid and potassium hydroxide. Starting materials in candidate smoke formulations were input into the code in their relative weight percentages. The chemical formula, heat of formation, state of matter {solid, liquid or gas} and density for each ingredient were also data inputs. Thermochemical runs were conducted at 1, 2 and 4 atmospheres.

It is informative to run the thermochemical code for the formulation alone as well as in the presence of air since afterburning has a great effect on obscurant performance. Thus, additional thermochemical runs were conducted with up to two parts by weight of air for every part of obscurant.

The thermochemical code can also be run in a mode where the chemical elements comprised in the composition can be heated or cooled to a specified temperature. This is very informative in the evaluation of obscurants since the products predicted to be formed at flame temperature can be allowed theoretically to cool to ambient temperature. Reactive species favored at high temperature decrease in prevalence or totally disappear. Condensable species that were liquids or gases at flame temperature condense into solids. Thus, the compositions of the solid

particulates that make up the obscurant smoke at ambient temperature are predicted as well as the resultant cooled gases, toxic or non-toxic.

Outputs from the model include the formulation density, equivalence ratio {Is the formulation fuel rich or fuel lean?}, combustion temperature and combustion products at each pressure input and at flame temperature or a given temperature input. Products predicted assume combustion is complete - no kinetic barriers are present to impede reactive intermediates from transforming into the most thermodynamically stable products at the stated temperatures and pressures. Data outputs of especial import for obscurant development are the flame temperature, the per cent solids, liquids, and condensable gases produced after combustion and cooling to ambient temperature. Liquids {at flame temperature} or condensible gases are very desirable for obscurant performance, e.g., $P_4O_{10}$ {sublimes at 573 K} or $HBO_2$ {melts at 509 K} since they will have a propensity to condense into finely divided particles having high surface area allowing efficient dispersion and reactivity/absorption with water vapor.

### 4.2 Preliminary Environmental and Human Health Assessment

Formulations were identified that produce a high percentage of solids, particularly hygroscopic solids that are gases or liquids at flame temperature. The combustion products predicted to be produced were analyzed for environmental and human health impacts as prescribed in Section 6.4.3 of ASTM E2552-08 (10) using the resources provided by the National Institute of Health in the ToxNet database (11). Although the NASA Lewis Thermochemical Code will not predict all products produced by incomplete combustion of the potential obscurant, these products of incomplete combustion were predicted through chemical intuition and comparison of similar systems. In this manner, formulations producing combustion or partial combustion products with less than desirable environmental and human health impacts were eliminated from further consideration before the Testing phase {ASTM E2552-08 Section 6.4 in reference (10)}.

### 4.3 Compatibility Testing

Differential Scanning Calorimetry {DSC} is used as a screening tool for assessing the thermal compatibility of materials and will only identify gross incompatibilities of mixtures. If a binary mixture exhibits shifts to lower temperatures for any exothermic event {relative to the temperatures for the single ingredient}, or if additional exothermic events are observed for a binary mixture, the material may be thermally incompatible. DSC samples were loaded in Seiko aluminum capsules. The capsules were heated from ambient to 350 °C at a rate of 20 °C /minute using a Mettler 821e DSC. Experiments were carried out under a 60 ml/minute nitrogen purge. Prior to testing, an indium sample loaded in a Seiko aluminum capsule was run to calibrate the temperature and heat flow of the DSC.

DSC will not identify any slow autocatalytic adverse interactions of materials. Vacuum Thermal Stability {VTS} testing which is essentially an elevated temperature isothermal “aging” technique will identify these types of interactions. Samples were loaded in VTS tubes; evacuated; and initial temperatures were recorded. The tubes were placed in a heating block maintained at 120 °C. After 48-hours, the tubes were removed; allowed to cool to room temperature; and final pressure readings and visual observations were recorded.

### 4.4 Speed Mixing

The FlackTec Inc. SpeedMixer is a dual asymmetric centrifugal laboratory mixer {Figure 1}. Ingredient powders to be blended are weighed into a plastic mixing cup. A lid is screwed onto the cup, the cup placed into an appropriately sized cup holder, which, in turn, is placed into the sample holder in the SpeedMixer mixing compartment. The lid to the mixing compartment is closed and the SpeedMixer is operated remotely. Ten gram samples were blended to obtain material for hazard sensitivity tests whereas sixty gram samples were blended to produce material for performance and effluent toxicity testing. The mix procedure consisted of three separate mix cycles at 3540 rpm {maximum blending speed} for 15 seconds. If the temperature of the blended powder exceeded 165 °F after either the first or second mix cycle due to frictional heating during the mixing process, the powder was allowed to cool to below 120 °F before proceeding with the next mix cycle.


**Figure 1: FlackTek SpeedMixer {left}, mixing cup {center}, SpeedMixer mixing compartment with mixing cup placed cup holder system {right}**

### 4.5 Hazard Sensitivity Testing

Sensitivity of energetic samples to impact stimuli was determined using a Modified Bureau of Mines Impact Machine more commonly known as the ABL Impact machine. A 2 kg weight is released from an electromagnet at a prescribed height above a sample placed between a circular hammer and anvil. The operator determines if the sample initiated or not. The initiation frequency is determined as a function of the drop height. In this study, impact sensitivity was determined either by a limit test or a threshold initiation level {TIL}. In the limit test, samples are tested at a drop height of 6.9 cm. If samples of a given formulation do not initiate after 20 replications, the formulation is deemed acceptable for mixing and testing without further management review and approval. Testing by the TIL method commences by dropping the impacting weight from successively higher predetermined heights and continuing at each level until an initiation is observed. At this point, the drop height for the 2 kg weight is lowered by

**Figure 2: ABL Impact Machine**

one or two intervals and the test is repeated as above. Testing is continued until twenty failures are obtained for a given drop height one level below that at which an initiation was obtained. This drop height is then recorded as the TIL. If the TIL is below 6.9 cm, management review and approval will be required before further development of that formulation can continue.

Sensitivity of energetic samples to friction stimuli was determined using the ABL Sliding Friction test {Figure 3}. Friction is produced by sliding a steel wheel over a steel plate. The sample being tested is placed at the interface between the wheel and plate. A load is applied to compress the sample. The test is conducted by sliding the plate under the fixed wheel. Plate travel is 1.0 inch. Each time a test is conducted, the wheel is moved to a fresh wheel and plate surface. Both are ground perpendicular to the direction of travel to a surface finish of 125 microns to provide consistency. The wheel is nominally 2.0 inches in diameter and 0.125 inches thick. The steel is hardened to a Rockwell AC @ 40-50 hardness. The plate is 2.25 inches wide and 6.5 inches long and hardened to a Rockwell AC @ 58-62 hardness. A TIL level is determined from this test in the same manner as the ABL impact test using load on the sample and plate velocity as variables. Tests start at 8 feet per second and 800 lbs wheel load. If no fires occur after 10 trials, results are reported > 800 lbs @ 8 ft/sec. If fires occur, tests are performed at 660 lbs at 8 ft/sec, 560 lbs at 8 ft/sec, etc. decreasing load until 25 lbs is reached. If fires are still occurring within 20 trials, tests continue at 6 ft/sec first at 800 lbs and then at gradually decreasing loads. Tests do not go to a lower velocity until all loads at the current velocity are tested. Tests continue at successively lower velocities and loads until 20 no-fires are obtained. The limit test was conducted at 40 lbs @ 3 ft/sec.

**Figure 3: ABL Friction Machine**

The primary parts of the ABL ESD test apparatus {Figure 4} are a sample cup, a discharge needle, and a capacitor bank to provide the electrical energy (12). A pyrotechnic sample is tested by placing it in the sample cup, which is grounded to a base plate. The capacitor bank is charged to 5000 volts. The desired energy is determined by selecting a capacitance value from the capacitor bank. The test is then initiated by dropping the discharge needle rapidly toward the sample. The electrical discharge between the needle and the ground passes through the sample. This test simulates conditions in processing where an electrical discharge could take place as electrostatic energy builds up on process equipment or operators as they move about. Limit tests were conducted at 0.075 J. The TIL method was conducted using a procedure similar to that for ABL impact.


**Figure 4: ABL ESD test apparatus {12}, close-up view of the ESD needle, stand and sample enclosure {right}**

The Simulated Bulk Autoignition Test {SBAT} simulates the thermal response of a bulk sample when heated in the presence of air. It is designed {Figure 5} to detect the bulk heating effect while using relatively small test samples, ≈5 g. The test apparatus for the SBAT consists of a ten inch diameter by six inch high aluminum cylinder. The cylinder has six flat bottom holes, or cells, drilled in a radial pattern with a heating element located in the center. The entire unit is surrounded by insulation. Glass test tubes hold the test sample and are placed in a cell within the cylinder. Tests are conducted at ambient pressure. Insulated test samples are heated in an aluminum thermal mass, and their temperatures are compared to an identically insulated, non-reactive sample. When a test sample experiences an endotherm, its temperature falls behind that of the inert sample, resulting in a negative differential temperature between the test sample and the inert sample. When the test sample experiences an exotherm its temperature rises above that of

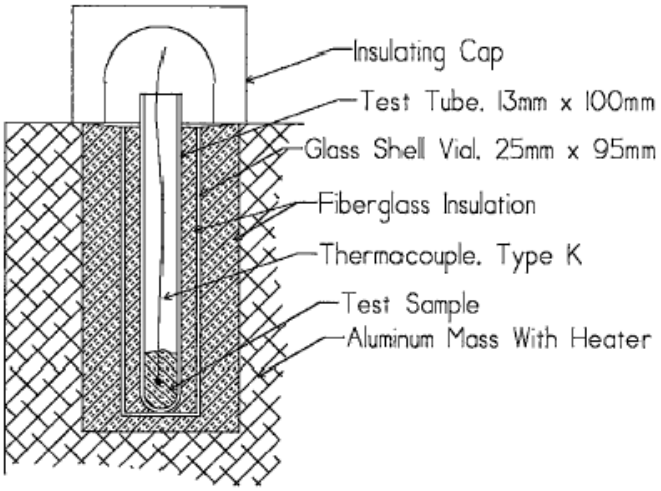


**Figure 5: Diagram of an SBAT cell**

the inert sample, resulting in a positive differential temperature between the test sample and the inert sample. Samples are heated at a ramp rate of 24 °F/hour up to 500 °F. Samples with exothermic onsets below 225 °F are considered thermally unstable. ATK management approval must be obtained before further development efforts may occur for such thermally unstable compositions.

### 4.6 Pressing of Dry Blended Obscurant Samples

Dry blended obscurant samples were prepared for performance and smoke toxicity testing by pressing 0.5" diameter pellets with weights ranging from 1-8 grams at 1000 lbs load {5096 psi} for 60 seconds at ambient temperature in a stainless steel die and punch set on a Carver hand operated press {Figure 6}.

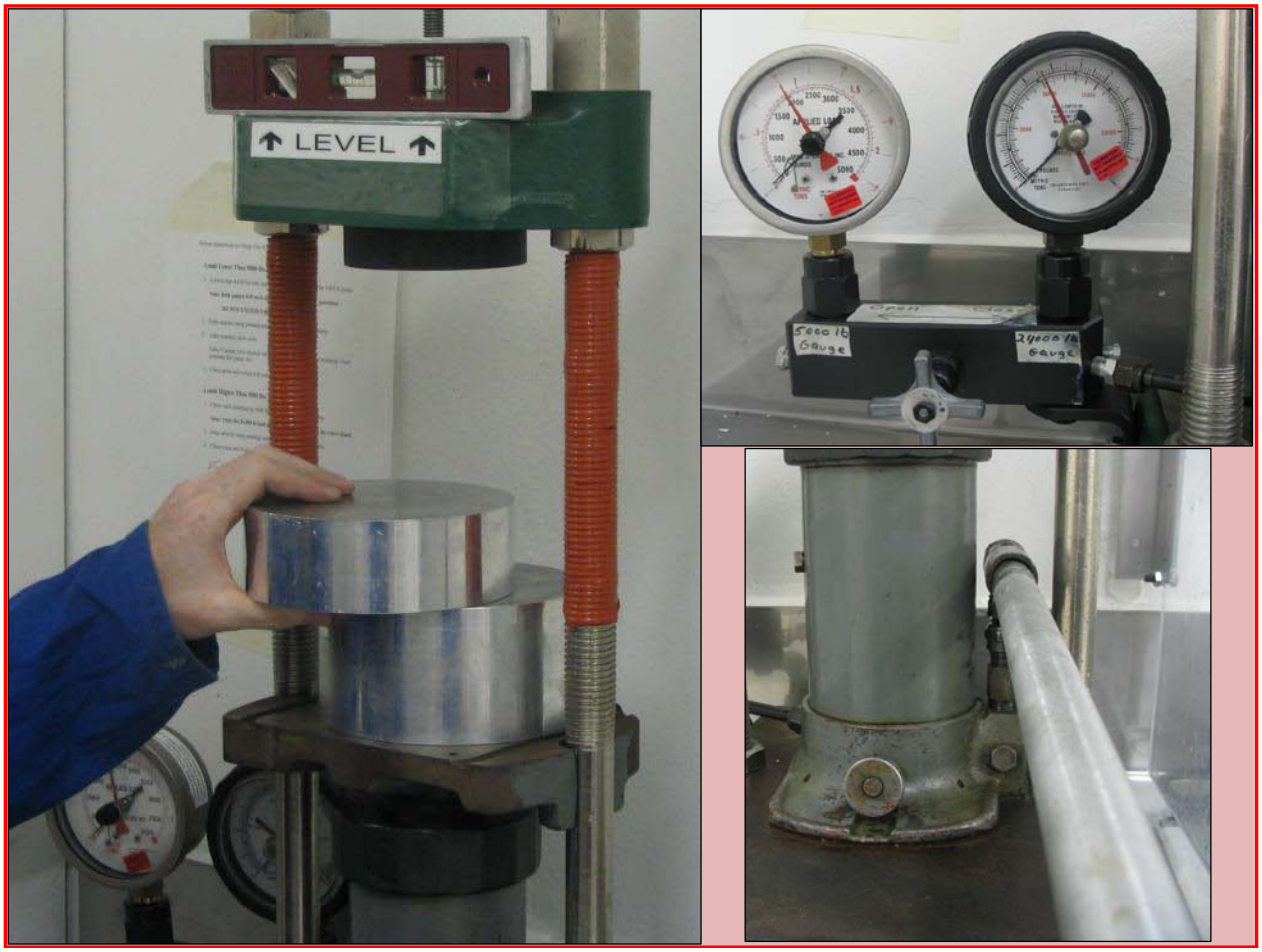


**Figure 6: Carver hand operated press: platen {left}, pressure gauges {top right}, hand operated pressure control system {bottom right}**

### 4.7 Initial Obscurant Formulation Screening

Up to five grams of obscurant in the form of blended powders, compressed 0.5" diameter pellets or excised, cured samples were ignited in an attended operation using a 0.75mm tungsten wire attached to a ≈2 foot ignition wand in a laboratory hood {Figure 7}. Voltage to the hot wire was controlled using a variable output, 6.3 VAC nominal power supply using 120 V input power. The 0.5" diameter pellets were bonded to roofing nails and placed in a solid metal sample holder

allowing ease of ignition. Samples were ignited with the hood exhaust system on or with it off momentarily allowing a better assessment of the smoke produced before it was removed from the hood area with the exhaust system.


**Figure 7: Test equipment used for initial obscurant formulation screening. Hood designated for ignition and combustion characterization of 0.05-5.0 grams of pyrotechnics {left}, variable output power supply {top right}, sample holder and ignition wand with tungsten ignition wire {bottom right}**

### 4.8 Obscurant Analysis in the 100 Cubic Foot Chamber

Transmittance measurements were conducted in a stainless steel 100 cubic foot chamber located in ATK Propulsion System's I-10N facility {Figure 8}. The chamber includes a full size door in front for ease of access and cleaning of the chamber. The door has an eye level observation window allowing real time observation of sample ignition and smoke dispersal. The door is sealed using threaded tightening clamps and a gasketed entryway.

The ignition power source is identical to that used for hood testing {Figure 7, top and bottom left}. The 0.5" diameter pellets were bonded to roofing nails and placed in a solid metal sample holder allowing ease of ignition {Figure 9}. These pellets were ignited remotely. A thick copper tensioning wire assists in positioning and assuring good contact of the Alfa Aesar 0.75mm 99.95% metals basis tungsten wire with the top of an obscurant pellet.

The 150 watt, SL-150 Zoo Med Basking Spot Lamp light source on the right side of the chamber illuminates the obscurant smoke through a quartz window. Light intensity data is collected through a quartz window on the opposite face of the chamber by an International Light model SED033 with the /Y photopic filter. The sensor is connected to an SRS model SR570 current amplifier. The voltage output of the amplifier is recorded using a Nicolet Sigma 100 oscilloscope. Data was recorded at 50 ms/ point for 27000 points.

Sample ports on the left side of the chamber allowed for particulate collection and gas sampling. Once obscurant smoke transmittance, particulate and toxic gas data were collected, the smoke was swept from the chamber by turning on the elephant trunk exhaust system attached to the top vent on the 100 cubic foot chamber. The vent valve is then opened. A handle is attached to the vent valve allowing ease of operation at floor level. Next, the air inlet port {Figure 8, top center} is opened allowing air flow into the chamber and out flow of the obscurant smoke through the elephant trunk. The main door to the 100 cubic foot chamber was not opened until transmittance in the chamber was well above 90% and carbon monoxide levels were well below 35 ppm. At that point the elephant trunk exhaust system was shut down. The I-10N facility also includes a roof exhaust system. The roof exhaust system was kept on at all times during obscurant testing to assist in removal of small amounts of particulate or toxic gases that may have leaked from the chamber during transmittance, particulate and toxic gas measurements. The quartz windows used for transmittance measurements were cleaned periodically to remove particulates that may have settled on them during testing. After each day of testing, the inner surfaces of the test chamber were thoroughly cleaned with wipes and window cleaner to mitigate corrosion of said surfaces.

Representative voltage vs. time traces collected for the four formulations tested in the 100 cubic foot tank are shown in Figure 10. The first portion of each trace is the time between pellet ignition and when the smoke is evenly dispersed in the path between the light source and detector. Typically, several hundred seconds are required to obtain a stable transmittance signal. Transmittance readings reported below were measured after the transmittance has stabilized. The abrupt rise in voltage {increasing transmittance} observed on the right side of the trace occurs when the smoke is swept from the chamber using the elephant trunk exhaust system with the air inlet port open.

**Figure 8: Obscurant 100 cubic foot test chamber {left}, light source for transmittance measurements {bottom right}, light detector, air inlet and gas sampling ports {top center}, pellet ignition system {top right}**


**Figure 9: HCE obscurant replacement samples prepared for testing {left}, pellet ready for igntion {right}**

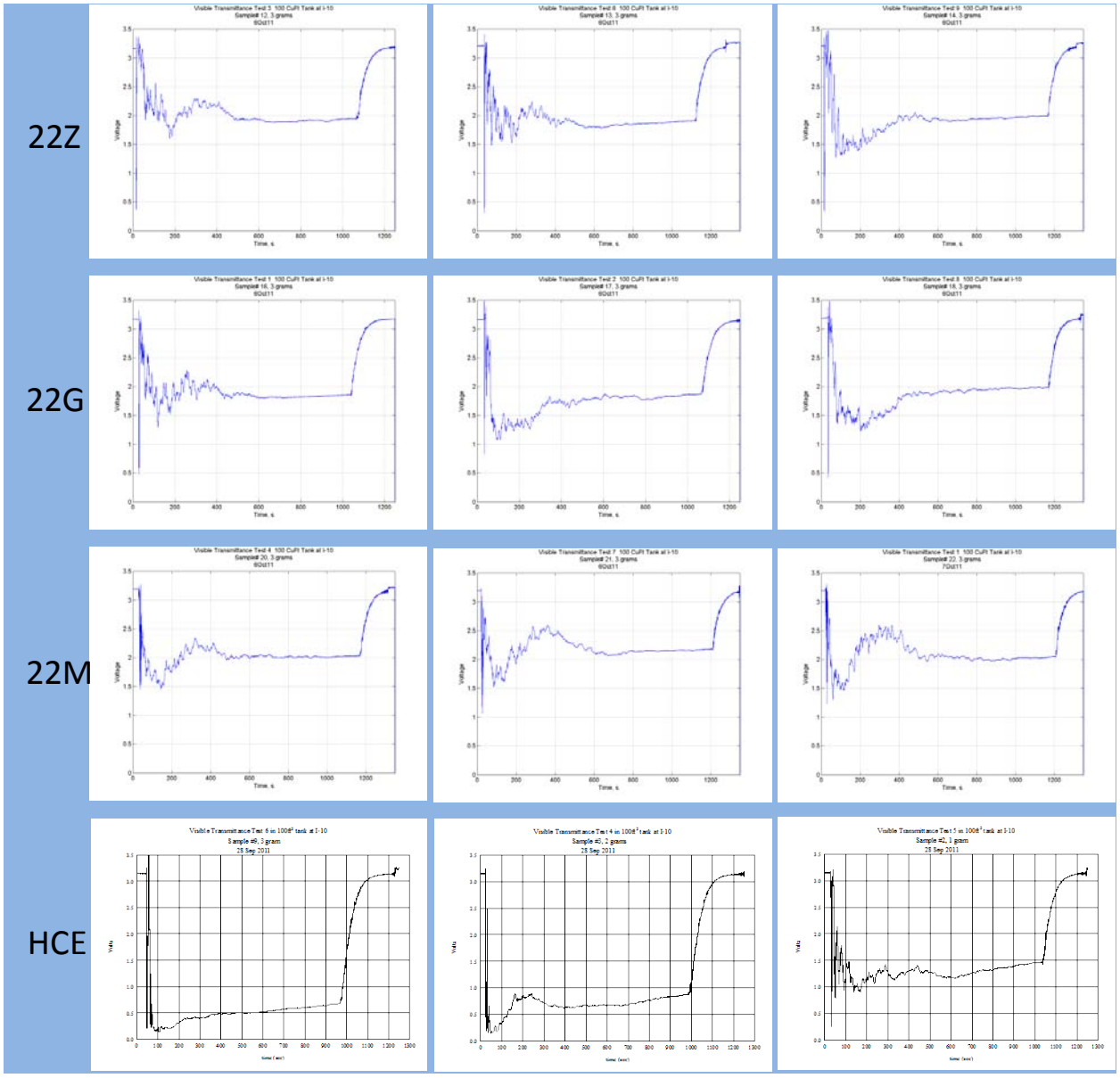


**Figure 10: Representative voltage {voltage is proportional to transmittance} vs. time curves obtained from 100 cubic foot chamber tests on 3 gram pellets of HCE obscurant replacement formulations; 22Z, 22G and 22M; as well as corresponding traces for 3 grams {bottom left}, 2 grams {bottom middle} and 1 gram {bottom right} of HCE obscurant. Voltage values range from 0.0 to 3.5 volts. Time values range from 0 to 1200 seconds.**

Methods for detecting toxic gases are summarized in Table 1. Directions accompanying the Draeger tubes were followed prescribing the number of pumps of the Draeger tube bellows {Figure 11} that are required for measurements of the gases in a given concentration range. The Draeger Chip Measurement System {CMS} was used to not only measure phosgene levels in the 100 cubic foot chamber but also phosgene levels outside of the chamber while the properties of HCE smokes were being monitored inside the chamber. No detectable levels of phosgene, >0.05 ppm, were detected outside of the chamber. Likewise, the iBRID MX6 multi-gas monitor was used to detect carbon monoxide levels inside and outside of the chamber during testing as well as

while the chamber was flushed of obscurant effluents. Again, no detectable levels of carbon monoxide, >1 ppm, were detected outside of the chamber. Use of the iBRID MX6 multi-gas monitor was discontinued as a means of measuring carbon monoxide levels in the chamber because the obscurant particulates tended to clog up the detection system.

**Table 1: Toxic gases analyzed and method for their detection**

| Toxic gas | Detection Method |
|---|---|
| Hydrogen Chloride | HCl 0.2/a Draeger Tube |
| Carbon Monoxide, Peak | iBRID MX6 multi-gas monitor |
| Carbon Monoxide, Equilibrated | iBRID MX6 multi-gas monitor |
| Carbon Monoxide, Equilibrated | CO 10/b Draeger Tube |
| Nitrous Gases, $NO_2$ and NO | Nitrous Gases, 20/a Draeger Tube |
| Chlorine | Chlorine, 0.2/a Draeger Tube |
| Ammonia | Ammonia, 5/a Draeger Tube |
| Phosgene | Draeger Chip Measurement System, Phosgene, 0.05-2.0 ppm |

**Figure 11: Gas monitoring devices: Draeger Tube Bellows {left}, Draeger CMS with ten chemical specific chips {center}, iBRID MX6 multi-gas monitor {right}**

### 4.9 Particulate and Toxic Gas Analysis at Autoliv Americas

Three gram, 0.5" diameter pellets {Section 5.6} of baseline and obscurant candidate samples were provided to Autoliv Americas to obtain additional toxic gas analysis data (13) and to determine particulate concentration, particulate particle size distribution as well as chemical analysis of the respirable particulate (14).

#### 4.9.1 Ignition

Different solid formulations of smoke obscurants in the form of three-gram 0.5" diameter pellets were placed inside a 100-$ft^3$ steel test tank {Figure 12-left}. The method of pellet ignition was very similar to that described in Section 5.8: An ATK power supply was connected to a 0.75mm tungsten wire, which was set on the surface of the solid. Current was applied until the material ignited, after which the power supply was shut off.

### 4.9.2 Gas Sampling and Analysis

Gases were sampled through a glass fiber filter and pumped directly into a Thermo Nicolet 6700 infrared spectrometer {cell path length of 10 meters, Figure 12-right} 1, 5, 10, 15, and 20 minutes after ignition. A blank air sample was also collected and analyzed before each test. Typical combustion byproducts were determined. The pump used for gas transfer was a bellows pump from Senior Flexonics.

Time weighted average concentrations were computed by weighting the sample concentration measured at each time based on the time between it and the previous sample. These average concentrations were then normalized to standard pressure {1 atm}. This normalization causes the concentrations to be slightly lower than those directly measured because more air would be in the tank to dilute the gases generated by the smoke obscurant were the test done at sea level.

Carbon monoxide and carbon dioxide were commonly seen at low concentrations at the earlier sampling times. Nitrogen oxides were also detected for some formulations.


**Figure 12: Autoliv test equipment: 100 cubic foot chamber {left}, FT-IR {right}**

### 4.9.3 Total Particulate Sampling and Analysis

Particulate was pumped at 5 L/min through 90 mm diameter Pall type A/E filters having a 1 micron pore size for 20-minutes. The pump used for total particulate collection was a bellows pump from Senior Flexonics. Particulate on the filters was weighed to determine the total airborne particulate concentrations.

### 4.9.4 Particulate Size Distribution Measurements

Particulate was also sampled with an inertial impactor to determine its aerodynamic particle size distribution. The inertial impactor was an Andersen 1 ACFM Non-Viable Ambient Particle Size Sampler {Figure 13} sold by Graseby Andersen. The particulate was sampled for 5 min, beginning 10 min after ignition. Even using this short sampling time, impactor plates were overloaded in some of the tests. The pump attached to the inertial impactor was a Gast pump,

model 1531-107B-G557X. The Andersen back-up filters were 81-mm diameter, grade 934-AH with a reported pore size of 1.5 microns.


**Figure 13: Andersen particulate particle size sampler**

The delayed particulate sampling resulted in slightly lower total particulate concentrations reported for the inertial impactor as compared with the total particulate filter. Comparisons of these data can be used to provide insight into how much particulate settles out or adheres to tank surfaces during the first 10 min.

4.9.5 **Chemical Analysis of Respirable Particulate**

Material on impactor plates representing particulate less than 3.3 μm in size was rinsed through a filter with deionized water. The water-soluble portions of these samples were analyzed for anions as well as ammonium and cesium cations by ion chromatography {IC} and multiple elements by inductively coupled plasma atomic emission spectrometry {ICP AES}. The anions were analyzed using a Dionex ICS-90 ion chromatograph whereas the cations were analyzed by a Dionex ICS2100 IC system with a CS12A column set. The ICP AES was a Thermo Jarrell Ash IRIS using form element analysis. It is an echelle spectrograph with a charge injection device camera.

The water-insoluble portions of the samples that were collected in the filters were washed with a 50% *aqua regia* solution. The acid-soluble filtrates of these samples were analyzed by the same ICP AES system.

## 5.0 RESULTS AND DISCUSSION

### 5.1 Silicon Based Obscurant Candidates

#### 5.1.1 Thermochemical Modeling

Thermochemical calculations were conducted on potential HCE smoke replacement formulations. The initial formulation family modeled was one with three ingredients, sodium nitrate, silicon powder and poly{dimethylsiloxane}, i.e., silicone polymer. The goal in this formulation effort was to produce a smoke producing partially hydrated sodium silicates. For example, $Na_2SiO_3$, is known to form a nonahydrate: it complexes as many as nine water molecules. Thus, a formulation that produces $Na_2SiO_3$ in combination with less than nine mole equivalents of water would seem optimal. The finely divided particulate will then have the capability of absorbing additional moisture in the air similar to zinc chloride and phosphoric acid producing a desirable smoke particulate. The baseline HCE formulation is fuel rich, it has an equivalence ratio of 1.60 where a value of 1.00 is neither fuel rich or lean {stoichiometric} and equivalence ratios below 1.00 are fuel lean. Thus, initial thermochemical calculations were conducted on formulations near an equivalence ratio of 1.6 with varying mole ratios of air added to determine their effect on temperature.

The results of these thermochemical modeling calculations, summarized in Table 2, suggest these formulations burn very hot, require oxygen from the air to be completely combusted and will start to cool significantly in the presence of excess air. If the goal is to produce sodium silicates that are more hygroscopic than silica, more sodium based ingredients need to be incorporated into the formulation. The amount of carbon dioxide produced should also be considered when assessing the merits of a given formulation. Some carbon dioxide will help disseminate the smoke whereas too much will decrease smoke efficiency and produce a too diffuse plume of smoke.

Two formulation approaches were considered during this development:

1. **Silicone Grease:** Formulations with relatively low silicone levels were considered where the silicone polymer would be integrated into the formulation as vacuum grease blended in with sodium nitrate and higher percentages of silicon powder. Formulations 16H and 20B were selected for experimentation. Formulation 16H combusts to produce a higher concentration of the sodium rich $Na_2Si_2O_5$ which should nucleate more readily with water whereas 20B is predicted to produce more solid particulate and less carbon dioxide.
2. **Curable RTV Silicone:** Formulations with higher silicone polymer levels sufficient to produce uncured formulations with acceptable viscosities for casting into a grain. These formulations produce significantly higher levels of carbon dioxide than those with 5-10% silicone grease. They also produce more water vapor that could immediately complex with the sodium silicates. Formulations 16K and 16D were selected for experimentation. 16K is predicted to form higher amounts of $Na_2Si_2O_5$ upon combustion whereas 16D produces less carbon dioxide and water.

**Table 2: Exemplary thermochemical calculations on potential HC smoke replacement formulations containing silicon. Formulations selected for experimentation are in bold.**

| HCEsub ID# | Formulation | Fuel to Oxidizer Ratio | Pyro/Air Ratios: Flame Temp. {K} at 1000 psi | Pyro/Air Ratios: Residual Wt. Fraction of $O_2$ | Mole Ratio of Predicted Combustion Products | Gas Fraction {before after-burning} |
|---|---|---|---|---|---|---|
| 2519-16B | 59.0% Sodium Nitrate, 31.0% Silicon 10.0% Silicone | 1.697 | 1:0-3042, 1:1-3273, 1:2-2657 | 1:0-0.000, 1:1-0.017, 1:2-0.062 | 1.00 $Na_2Si_2O_5$ 1.50 $SiO_2$ 0.96 $H_2O$ 0.64 $CO_2$ | 0.532 |
| 2519-16C | 59.5% Sodium Nitrate, 20.5% Silicon, 20.0% RTV | 1.784 | 1:0-2978, 1:1-2974, 1:2-2670 | 1:0-0.000, 1:1-0.011, 1:2-0.058 | 1.00 $Na_2Si_2O_5$ 0.72 $SiO_2$ 1.90 $H_2O$ 1.27 $CO_2$ | 0.502 |
| **2519-16D** | **60.0% Sodium Nitrate, 10.0% Silicon, 30.0% RTV** | **1.86** | **1:0-2959, 1:1-2616, 1:2-2373** | **1:0-0.000 1:1-0.005, 1:2-0.060** | **1.00 $Na_2Si_2O_5$ 0.05 $Na_2SiO_3$ 2.97 $H_2O$ 1.98 $CO_2$** | **0.445** |
| 2519-16E | 59.0% Sodium Nitrate, 31.0% Silicon Powder 10.0% Silicone | 1.374 | 1:0-3403, 1:1-2818, 1:2-2557 | 1:0-0.001 1:1-0.051, 1:2-0.092 | 1.00 $Na_2Si_2O_5$ 0.58 $SiO_2$ 0.87 $H_2O$ 0.58 $CO_2$ | 0.510 |
| 2519-16F | 66.6% Sodium Nitrate, 13.4% Silicon, 20.0% RTV | 1.436 | 1:0-2931, 1:1-2804, 1:2-2170 | 1:0-0.000 1:1-0.049, 1:2-0.100 | 1.00 $Na_2Si_2O_5$ 0.27 $Na_2SiO_3$ 2.16 $H_2O$ 1.44 $CO_2$ | 0.585 |
| 2519-16G | 68.0% Sodium Nitrate, 2.0% Silicon, 30.0% RTV | 1.487 | 1:0-2865, 1:1-2297, 1:2-1763 | 1:0-0.000 1:1-0.058, 1:2-0.107 | 0.01 $Na_2Si_2O_5$ 1.00 $Na_2SiO_3$ 2.52 $H_2O$ 1.63 $CO_2$ | 0.532 |
| **2519-16H** | **74.3% Sodium Nitrate, 15.7% Silicon, 10.0% Silicone** | **1.00** | **1:0-2805, 1:1-2464, 1:2-1864** | **1:0-0.056 1:1-0.116, 1:2-0.161** | **1.00 $Na_2Si_2O_5$ 0.87 $Na_2SiO_3$ 1.42 $H_2O$ 0.95 $CO_2$** | **0.587** |
| 2519-16I | 78.0% Sodium Nitrate, 2.0% Silicon, 20.0% RTV | 1.00 | 1:0-2296, 1:1-1642, 1:2-1306 | 1:0-0.093 1:1-0.147, 1:2-0.165 | 1.00 $Na_2Si_2O_5$ 0.57 $Na_2CO_3$ 2.47 $H_2O$ 0.95 $CO_2$ | 0.574 |
| 2519-16J | 78.5% Sodium Nitrate, 0.0% Silicon, 21.5% RTV | 1.00 | 1:0-2191, 1:1-1534, 1:2-1220 | 1:0-0.100 1:1-0.151, 1:2-0.167 | 1.00 $Na_2Si_2O_5$ 0.93 $Na_2CO_3$ 3.00 $H_2O$ 1.06 $CO_2$ | 0.542 |
| **2519-16K** | **65.0% Sodium Nitrate, 5.0% Silicon, 30.0% RTV** | **1.618** | **1:0-2930, 1:1-2589, 1:2-1999** | **1:0-0.000 1:1-0.034, 1:2-0.090** | **0.51 $Na_2Si_2O_5$ 1.00 $Na_2SiO_3$ 3.93 $H_2O$ 2.62 $CO_2$** | **0.492** |
| 2519-20A | 72.0% Sodium Nitrate, 25.0% Silicon, 3.0% Silicone | 0.994 | 1:0-3847, 1:1-2983, 1:2-2271 | 1:0-0.045, 1:1-0.094, 1:2-0.133 | 1.00 $Na_2Si_2O_5$ 0.18 $SiO_2$ 0.23 $H_2O$ 0.16 $CO_2$ | 0.391 |
| **2519-20B** | **72.5% Sodium Nitrate, 22.5% Silicon, 5.0% Silicone** | **1.002** | **1:0-3791, 1:1-2859, 1:2-2169** | **1:0-0.045, 1:1-0.098, 1:2-0.136** | **1.00 $Na_2Si_2O_5$ 0.01 $SiO_2$ 0.39 $H_2O$ 0.26 $CO_2$** | **0.387** |

### 5.1.2 **Ingredient Compatibilities**

Before the down selected formulations could be mixed, compatibilities of the various ingredients needed to be determined (15). Thus, compatibility testing was performed on sodium nitrate and

silicon with RTV-615A, RTV-615B, and Dow Corning high vacuum grease. RTV-615A and RTV-615B are the uncured components of a two-part curable silicone polymer.

Differential Scanning Calorimetry {DSC} experiments were conducted to identify gross incompatibilities of materials. Shifts in the onset and peak temperatures of the exothermic events for a material when tested with a second material may be indicative of thermally incompatible materials. Shifts to lower temperatures of 20 °C or more, or shifts to temperatures lower than 200 °C are red flags for incompatible materials. The DSC thermograms collected for this study are shown in Figures 14-16. Only the dimethylvinyl terminated silicone, RTV615A, exhibited a significant exotherm below 200 °C. The exothermic onsets for RTV615A alone and with sodium nitrate or silicon powder ranged between 176-187 °C. The shape of the thermal curve did not change or shift significantly to lower temperature upon addition of the second ingredient. These material pairs do not appear to be thermally incompatible.

Vacuum Thermal Stability {VTS} studies were conducted on the various material pairs. VTS is essentially an elevated temperature "aging" test, where materials are mixed and aged under vacuum. The volume of gas evolved during accelerated aging is then measured for each material alone and compared to that evolved for the blended material pair. From this data, a compatibility factor is calculated. Binary mixtures with compatibility factors less than 2.0 ml/g are classified as thermally compatible. Table 3 contains a summary of the VTS experimental data. Based on this data, sodium nitrate is thermally compatible with silicon powder, RTV-615A, RTV-615B, and with Dow Corning high vacuum grease. Silicon powder is also thermally compatible with RTV-615A, RTV-615B, and with Dow Corning high vacuum grease.

### 5.1.3 **Hazard Sensitivity Data**

Hazard sensitivity data for silicon/silicone/sodium nitrate based obscurant candidates are summarized in Table 4 (16). The data were collected on material blended in ten-gram Speed Mixes {see Section 5.4}. For cured energetic compositions, hazard sensitivity data are typically collected on both uncured and cured samples. Hazard sensitivity data were collected only on uncured samples of HCEsub-2519-16D. Data were collected on both uncured and cured HCEsub-2519-16K. All of the compositions showed minimal response to impact, friction and thermal stimuli. The compositions did show sensitivity to electrostatic discharge. In fact, the compositions containing high percentages of silicon powder and only 5-10% silicone vacuum grease were very ESD sensitive. Tested values are below those listed in the ATK Hazardous Operations Standard {AHOPS}. Thus, special management approval is required to handle these materials. Materials that have ESD sensitivity values below 0.075 J, the AHOPS standard, are tested for ignition by an 8 J spark in a bulk sample {a few grams} to determine if such a sample is consumed by the 8 J ESD event. In the case of HCEsub-2519-16H and HCEsub-2519-20B, a bulk sample was not consumed. The cured sample of "16K", having the least amount of silicon powder, is sufficiently insulative that an electrical spark does not travel through it.

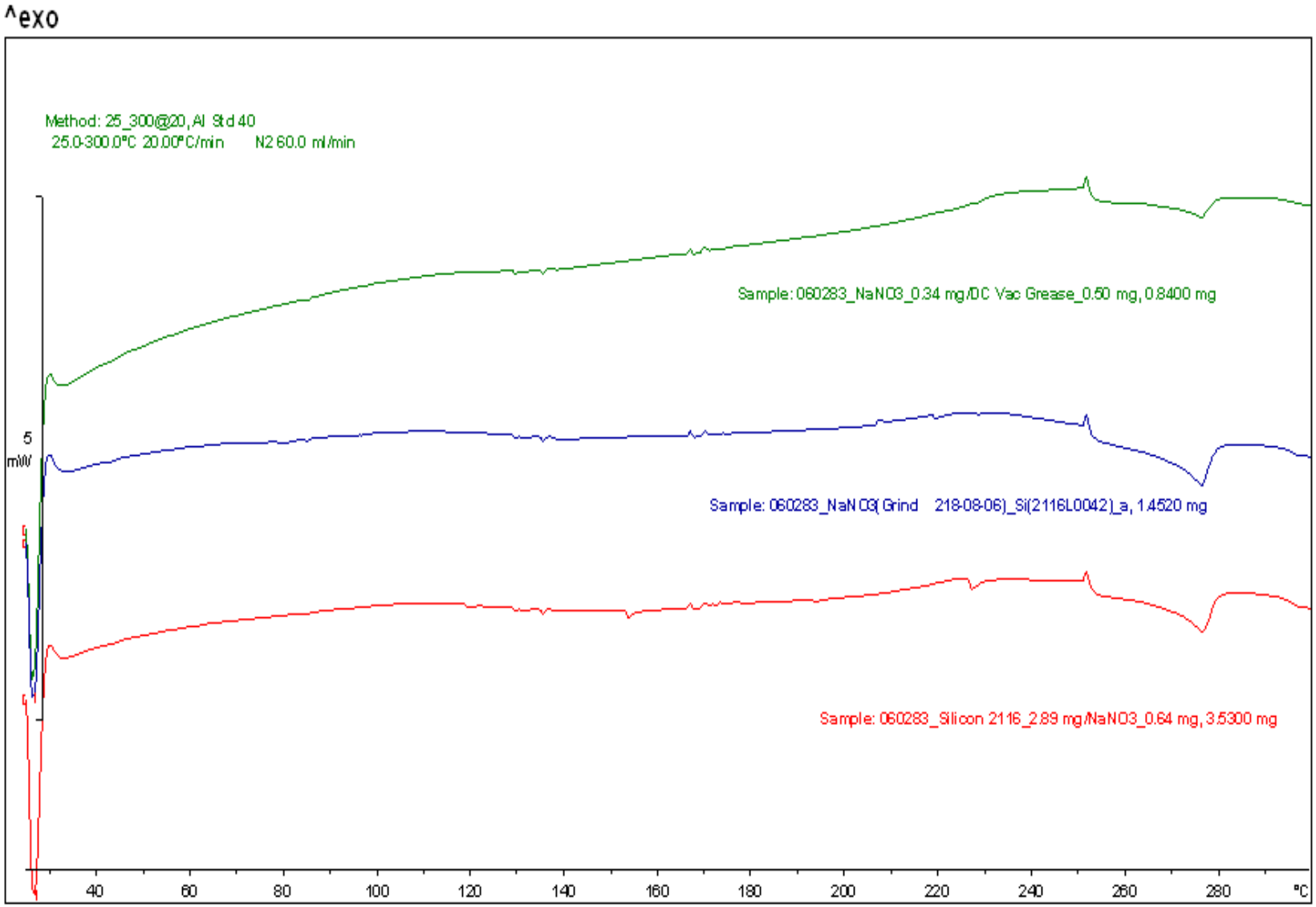


**Figure 14: DSC thermograms: sodium nitrate with Dow Corning silicone vacuum grease {green trace}; sodium nitrate with silicon powder {blue and red traces}. The bar along the y-axis is equivalent to 5 mW. Exothermic peaks are positive relative to baseline.**

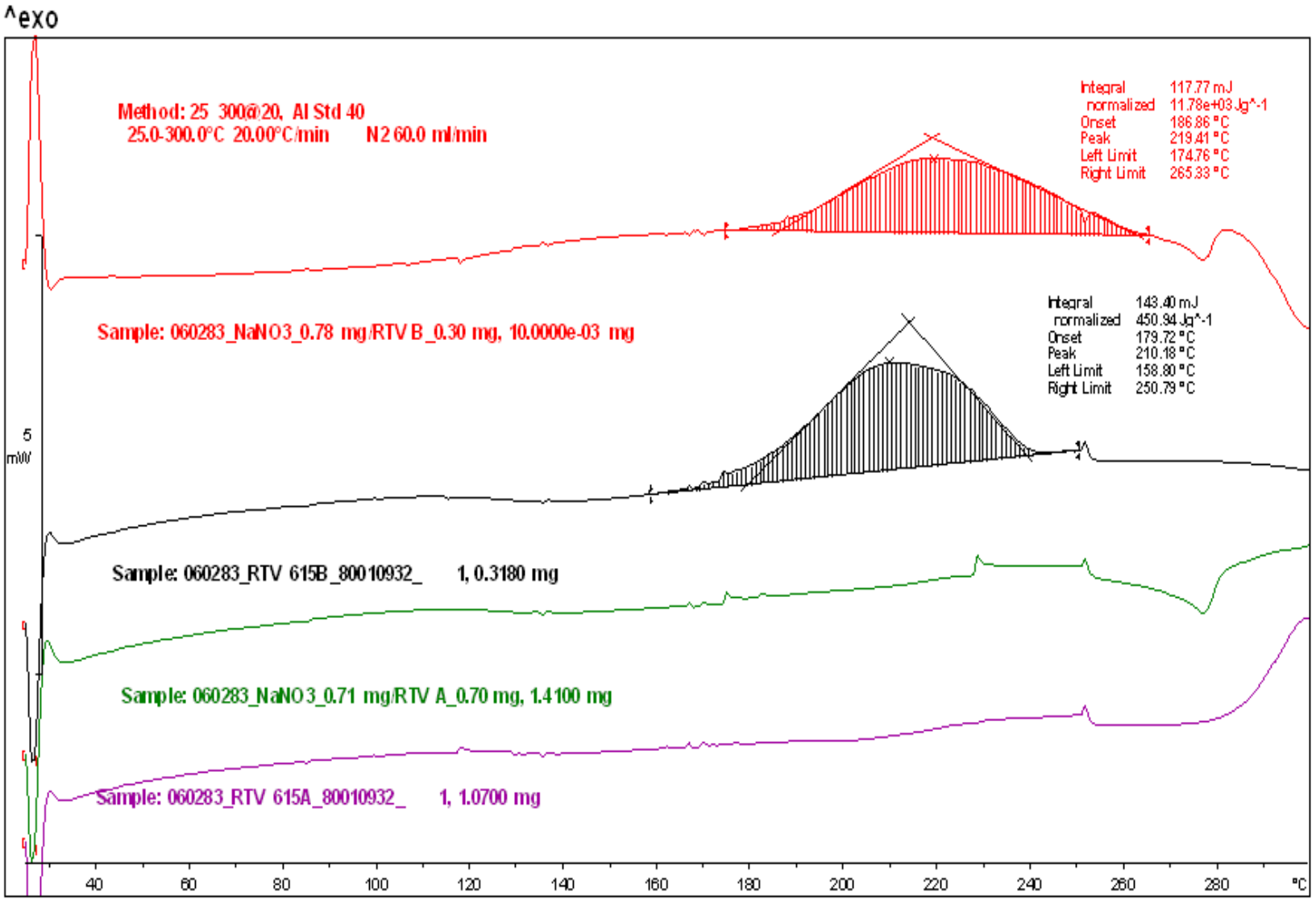


**Figure 15: DSC thermograms: sodium nitrate with RTV 615B {red trace}; RTV 615B alone {black trace}; sodium nitrate with RTV 615A {green trace}; RTV 615A alone {violet trace}. The bar along the y-axis is equivalent to 5 mW. Exothermic peaks are positive relative to baseline.**

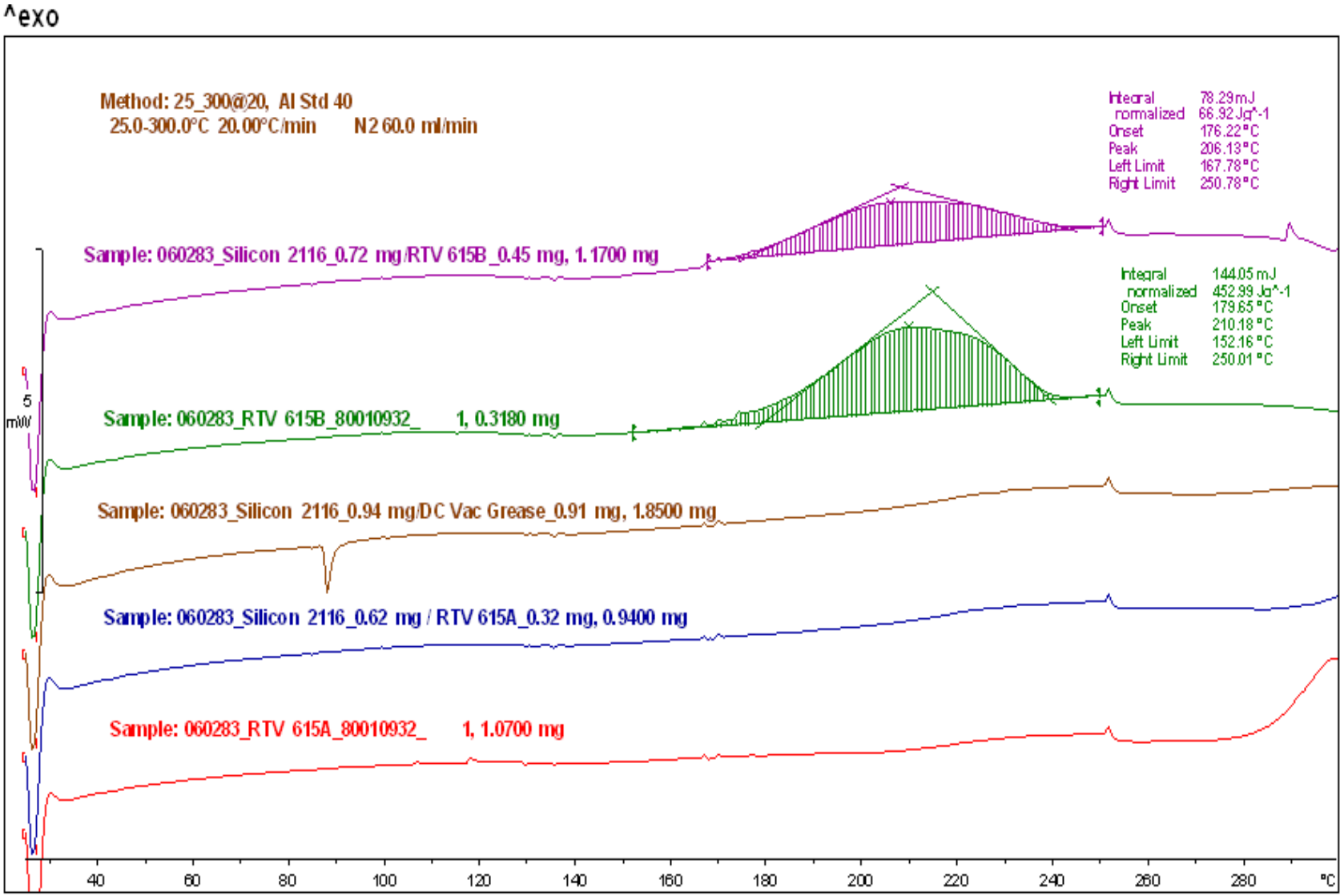


**Figure 16: DSC thermograms: silicon powder with RTV 615B {violet trace}; RTV 615B alone {green trace}; silicon powder with Dow Corning silicone vacuum grease {brown trace}; silicon powder with RTV 615A {blue trace}; RTV 615A alone {red trace}. The bar along the y-axis is equivalent to 5 mW. Exothermic peaks are positive relative to baseline.**

**Table 3: Summary of the VTS compatibility data for silicon based obscurant candidates**

| Materials | Volume of Evolved Gas | Compat-ibility Factor * | Comments |
|---|---|---|---|
| **NaNO3 Grind 218-008-06** | 0.383 ml/g<br>0.396 ml/g<br>**AVERAGE 0.381 ml/g** | **N/A** | |
| **Silicon 2116Lot#0042** | 0.375 ml/g<br>0.379 ml/g<br>**AVERAGE 0.377 ml/g** | **N/A** | |
| **RTV-615A** | 0.546 ml/g<br>0.501 ml/g<br>**AVERAGE 0.523 ml/g** | **N/A** | |
| **RTV-615B** | 3.701 ml/g<br>4.678 ml/g<br>**AVERAGE 4.190 ml/g** | **N/A** | |
| **Dow Corning High Vacuum Grease** | 0.422 ml/g<br>0.419 ml/g<br>**AVERAGE 0.421 ml/g** | **N/A** | |
| **Silicon/ RTV-615B** | 1.912 ml/g<br>1.790 ml/g<br>**AVERAGE 1.851 ml/g** | **-0.432 ml/g** | **Compatibility factor < 2.0 ml/g<br>Materials are thermally compatible** |
| **NaNO3/ RTV-615A** | 0.191 ml/g<br>0.216 ml/g<br>**AVERAGE 0.203 ml/g** | **-0.248 ml/g** | **Compatibility factor < 2.0 ml/g<br>Materials are thermally compatible** |
| **NaNO3/ RTV-615B** | 1.917 ml/g<br>2.471 ml/g<br>**AVERAGE 2.914 ml/g** | **0.629 ml/g** | **Compatibility factor < 2.0 ml/g<br>Materials are thermally compatible** |
| **NaNO3/ Dow Corning High Vacuum Grease** | 0.173 ml/g<br>0.159 ml/g<br>**AVERAGE 0.166 ml/g** | **-0.235 ml/g** | **Compatibility factor < 2.0 ml/g<br>Materials are thermally compatible** |
| **NaNO3/ Silicon** | 0.148 ml/g<br>0.152 ml/g<br>**AVERAGE 0.150 ml/g** | **-0.229 ml/g** | **Compatibility factor < 2.0 ml/g<br>Materials are thermally compatible** |
| **Silicon/ RTV-615A** | 0.171 ml/g<br>0.279 ml/g<br>**AVERAGE 0.225 ml/g** | **-0.225 ml/g** | **Compatibility factor < 2.0 ml/g<br>Materials are thermally compatible** |
| **Silicon/ Dow Corning High Vacuum Grease** | 0.203 ml/g<br>0.167 ml/g<br>**AVERAGE 0.185 ml/g** | **-0.214 ml/g** | **Compatibility factor < 2.0 ml/g<br>Materials are thermally compatible** |

*** Compatibility Factor = E – {{F +G}/2} where**
**E = Average Gas Evolution for the mixed material pair;**
**F = Average Gas Evolution for 1st material in study**
**G = Average Gas Evolution for 2nd material in study**

**Table 4: Hazard sensitivity data for silicon-based obscurant candidates**

| Material | STR Number | ABL ESD | Bulk ESD | ABL Friction | Impact | Autoignition {SBAT} |
|---|---|---|---|---|---|---|
| AHOPS Requirements | NA | > 0.075 J | NA | > 40 lbs @ 1 ft/sec | >7 cm {ABL} | >225 F |
| HCEsub-2519-16H 74.3% $NaNO_3$, 15.7% Si, 10.0% Silicone | 31126 | 0.009 J | No Consumption | >750 lbs @ 8 ft/sec | >80 cm | >500 ºF |
| HCEsub-2519-20B 72.5% $NaNO_3$, 22.5% Si, 5.0% Silicone | 31113 | <0.004 J | No Consumption | >750 lbs @ 8 ft/sec | >80 cm | >500 ºF |
| HCEsub-2519-16D, uncured 60.0% $NaNO_3$, 10.0% Si, 30.0% RTV-615 | 31112 | 3.054 J | Test Not Required | >750 lbs @ 8 ft/sec | >80 cm | >500 ºF |
| HCEsub-2519-16K, uncured 65% $NaNO_3$, 5.0% Si, 30.0% RTV-615 | 31124 | 0.133 J | Test Not Required | >750 lbs @ 8 ft/sec | >80 cm | >500 ºF |
| HCEsub-2519-16K, cured 65% $NaNO_3$, 5.0% Si, 30.0% RTV-615 | 31125 | Too insulative to test | NA | >750 lbs @ 8 ft/sec | >80 cm | >500 ºF |

### 5.1.4 Initial Formulation Screening

Material from the two ten-gram mixes allocated for each formulation, HCEsub-2519-16H, -20B, -16D and the four ten-gram mixes of -16K {cured and uncured}, were utilized for initial formulation screening {see Section 5.7}. The blended powders containing 5-10% Dow Corning vacuum grease, -16H and -20B, were pressed into 0.5" diameter four-gram pellets pressed at 500 lbs load. The uncured material from -16D and -16K was allowed to cure and samples thereof were ignited in the M-15A burn hood.

The formulations containing large quantities of silicon powder and smaller quantities of silicone vacuum grease, HCEsub-2519-16H and -20B, burned very brightly. Unfortunately, combustion produced little smoke and large quantities of slag that was not disbursed into the air. These formulations were eliminated from further consideration as replacements for HCE obscurant smoke.

The formulations containing the cast-cured RTV-615, HCEsub-2519-16K and -16D, produced more smoke and significantly less slag than those with more silicon powder and smaller amounts of silicone -16H and -20B. Of -16D and -16K, the former, containing 10% silicon powder instead of 5% silicon powder, appeared to produce the most smoke. This formulation {-16D} has a lower gas fraction. A greater proportion of its combustion requires afterburning with oxygen in the air: Its flame temperature is higher when allowed to burn in the presence two parts air for every part by weight of the obscurant relative to -16K {See Table 2}. Apparently, high sodium content in the combustion products is not important in smoke production at least in arid climates.

These data suggest that the best obscurant formulations in this family would be those that have higher silicon content in which only enough sodium nitrate is present to sustain combustion, e.g., 50.0% $NaNO_3$, 20.0% Si, 30.0% RTV-615 or 40.0% $NaNO_3$, 30.0% Si, 30.0% RTV-615. A point will be reached in which too much silicon powder is present. If the initial flame

temperature is too cool, slag formation may occur even with 30% of the RTV-615 gas generator present in the formulation. Cooler silicon particles dispersed by combustion gases may also quench in the cool air before they are fully combusted. Higher levels of silicon powder may prevent casting the curable formulations into a grain. However, many pyrotechnics with curable binders are pressed in the uncured state into grains instead of being cast. Press-cured formulations with 20.0% RTV-615 may combust without producing slag. Formulations HCEsub-2519-16H and -20B demonstrate that the presence of only 10% of the gas generating silicone polymer is insufficient to efficiently disperse combusted solids in the form of smoke.

#### 5.1.5 **Hundred Cubic Foot Chamber Tests**

In initial screening tests, existing candidate obscurant formulations containing boron appeared to produce more smoke than the silicon based candidates. So, although HCEsub-2519-16D was the most promising silicon based formulation, it was not down selected in the SEED phase of this program for testing in the hundred cubic foot chamber.

If further funding becomes available, a five point formulation matrix could be tested in the chamber to optimize smoke formation with the most promising formulation from this phase, HCEsub-2519-16D {#1}, at one corner:

1. 10% Si, 30% RTV-615, 60% NaN
2. 20% Si, 20% RTV-615, 60% NaN
3. 20% Si, 30% RTV-615, 50% NaN
4. 20% Si, 40% RTV-615, 40% NaN
5. 30% Si, 30% RTV-615, 40% NaN

### 5.2 Boron/Potassium Nitrate Based Obscurant Candidates

ATK participated in the development of the Improved Flash Bang Grenade, IFBG, in conjunction with NSWC Dahlgren and the Joint Non-Lethal Weapons Directorate. This grenade employs a flaked aluminum fuel and an igniter system containing a blend of magnesium/strontium nitrate and boron/potassium nitrate {BKN} igniter granules to produce a bright flash and a pressure impulse {bang}. In addition to these desirable effects, many early IFBG test articles containing large quantities of BKN produced a large amount of thick white smoke {Figure 17}. Liquids {at flame temperature} or condensible gases are very desirable combustion products that enhance obscurant performance, e.g., $P_4O_{10}$ {sublimes at 573 K} or $HBO_2$ {melts at 509 K}, since they will have a propensity to condense into finely divided particles having high surface area allowing efficient reactivity/absorption with water vapor. Most products predicted from the combustion of BKN are gaseous at flame temperature. This is a potential reason for the formation of the thick white smoke upon actuation of an IFBG.

**Figure 17: Test setup {left} and smoke output {right} of an IFBG containing an 18.2-gram net explosive weight shown two seconds after initiation of the grenade.**

In earlier obscurant development efforts at ATK, it was observed (17) that smokes containing potassium chloride acted as efficient obscurants. Potassium chloride condenses from the liquid state at 1043 K. Cesium chloride condenses at 918 K and ammonium chloride condenses from a gaseous state at 613 K. Because BKN burns very rapidly and its flame temperature is very high {2432 K}, candidate obscurant formulations were postulated where finely divided {-60 mesh} boron/potassium nitrate igniter granules are blended with one of the three aforementioned halide salts. The rationale is that the addition of halide salts to BKN decrease burn rate and lower flame temperature while vaporizing the halide salt enhancing the smoke output. The resulting obscurant effect would be derived from the condensation of vaporized halide salt and BKN combustion products. The following section describes activities conducted to characterize these families of obscurant candidates.

### 5.2.1 **Thermochemical Modeling**

Thermochemical calculations were conducted on potential HCE smoke replacement formulations based on a blend of BKN igniter with potassium chloride {Table 5} and cesium chloride {Table 6}.

In the cases of potassium chloride and cesium chloride, the ratio of BKN to the halide salt was varied. As expected, the flame temperature of the compositions decreased as the amount of halide salt added increased. The gas fraction at flame temperature is less than 1.00 because the formation of solid boron nitride is predicted. As the flame temperature decreases, other solids or liquids start to condense such as boron oxide, $B_2O_3$, potassium chloride and/or potassium borate, $K_2B_4O_7$. A larger mass of cesium chloride can be added to BKN relative to potassium chloride before condensation of boron oxide begins to become important. The trends suggest that maximum obscurant performance may initially increase with the addition of halide salt. However, addition of further amounts of halide salt coolant may promote formation of slag instead of smoke upon combustion of the compositions.

A small amount of hydrogen chloride formation is predicted at flame temperature. The amount present initially increases as the BKN/halide ratio increases, it peaks and then decreases. The decrease in hydrogen chloride at higher ratios is due to the lower flame temperature and decreasing importance of the $T\Delta S$ term in the Gibbs free energy equation, $\Delta G = \Delta H - T\Delta S$. This is further substantiated by the fact that as you allow the combustion products to cool to 700K using the NASA Lewis thermochemical code, hydrogen chloride disappears completely in the

BKN/CsCl family and is predicted at very low levels in the BKN/KCl family. One question that could be answered only by experimentation is if all the hydrogen chloride produced at flame temperature reacts with basic combustion products as the reaction products are cooled. Hydrogen chloride levels were measured in 100 cubic foot chamber tests and will be reported in Sections 6.2.5 and 6.2.6.

**Table 5: Thermochemical modeling of the BKN/KCl obscurant family**

| HCEsub ID | Halide/ BKN Ratio | Flame Temp. @ 1 atm (K) | Gas Fraction @ Flame Temp. | Wt Fraction at Flame Temp. | | | | | | Mass Ratio at 700 K | |
|---|---|---|---|---|---|---|---|---|---|---|---|
| | | | | KCl (G) | K2CL2 (G) | HCl (G) | KCl (L) | B2O3 (L) | K2B4O7 (L) | KCl/ K2B8O13 | HCl/ K2B8O13 |
| BKN | 0/10 | 2509 | 0.87 | 0.00 | 0.00 | 0.0000 | 0.00 | 0.00 | 0.00 | 0.00 | 0.00000 |
| 2519-22A | 1/10 | 2469 | 0.87 | 0.09 | 0.00 | 0.0006 | 0.00 | 0.00 | 0.00 | 0.18 | 0.00005 |
| 2519-22B | 2/10 | 2411 | 0.87 | 0.16 | 0.00 | 0.0011 | 0.00 | 0.00 | 0.00 | 0.35 | 0.00006 |
| 2519-22C | 3/10 | 2344 | 0.87 | 0.22 | 0.00 | 0.0016 | 0.00 | 0.00 | 0.00 | 0.53 | 0.00006 |
| 2519-22D | 4/10 | 2264 | 0.87 | 0.27 | 0.00 | 0.0021 | 0.00 | 0.00 | 0.00 | 0.71 | 0.00006 |
| 2519-22E | 5/10 | 2153 | 0.88 | 0.31 | 0.01 | 0.0020 | 0.00 | 0.00 | 0.00 | 0.88 | 0.00006 |
| 2519-22F | 7/10 | 1929 | 0.88 | 0.36 | 0.02 | 0.0021 | 0.00 | 0.01 | 0.00 | 1.24 | 0.00006 |
| 2519-22G | 10/10 | 1780 | 0.84 | 0.40 | 0.08 | 0.0008 | 0.00 | 0.05 | 0.00 | 1.77 | 0.00007 |
| 2519-22H | 12.5/10 | 1656 | 0.83 | 0.37 | 0.18 | 0.0003 | 0.00 | 0.06 | 0.02 | 2.21 | 0.00008 |
| 2519-22I | 15/10 | 1637 | 0.73 | 0.33 | 0.20 | 0.0002 | 0.06 | 0.03 | 0.09 | 2.65 | 0.00008 |

**Table 6: Thermochemical modeling of the BKN/CsCl obscurant family**

| HCEsub ID | Halide/ BKN Ratio | Flame Temp. @ 1 atm (K) | Gas Fraction @ Flame Temp. | Wt Fraction at Flame Temp. | | | | Mass Ratio at 700 K | |
|---|---|---|---|---|---|---|---|---|---|
| | | | | CsCl (G) | Cs2CL2 (G) | HCl (G) | B2O3 (L) | CsCl/ K2B8O13 | HCl/ K2B8O13 |
| BKN | 0/10 | 2509 | 0.872 | 0.00 | 0.000 | 0.00000 | 0.000 | 0.00 | 0.00000 |
| 2519-22T | 2.5/10 | 2442 | 0.887 | 0.15 | 0.000 | 0.00032 | 0.000 | 0.44 | 0.00000 |
| 2519-22U | 5/10 | 2366 | 0.898 | 0.28 | 0.000 | 0.00040 | 0.000 | 0.88 | 0.00000 |
| 2519-22V | 7.5/10 | 2285 | 0.906 | 0.38 | 0.001 | 0.00041 | 0.000 | 1.33 | 0.00000 |
| 2519-22W | 10/10 | 2195 | 0.913 | 0.46 | 0.002 | 0.00037 | 0.000 | 1.77 | 0.00000 |
| 2519-22X | 12.5/10 | 2076 | 0.918 | 0.52 | 0.005 | 0.00027 | 0.000 | 2.21 | 0.00000 |
| 2519-22Y | 15/10 | 1964 | 0.915 | 0.57 | 0.011 | 0.00015 | 0.011 | 2.65 | 0.00000 |
| 2519-22Z | 17.5/10 | 1925 | 0.903 | 0.60 | 0.016 | 0.00011 | 0.028 | 3.10 | 0.00000 |

At 700 K, the mass ratio of $K_2B_4O_7\{S\}$ to $K_2B_8O_{13}\{S\}$ remains constant at 0.84 for all BKN/CsCl and BKN/KCl formulations since the ratio of potassium nitrate to boron never changes. Obviously, the mass ratio of the halide salt to $K_2B_8O_{13}\{S\}$ will increase as more of the alkali metal halide coolant is added.

Formulations covering a broad range of BKN to halide salt ratios were selected for experimental evaluation {Table 7}. These formulations were selected to understand how the addition of halide salt to the BKN effects ignitability and burn rate as well the proportion of solids produced in the form of smoke relative to that produced in the form of a clinker or slag upon combustion of the obscurant candidate.

**Table 7: BKN/KCl and BKN/CsCl formulations selected for performance evaluation**

| Identification | Formulation |
|---|---|
| HCEsub-2519-22T | 80.0% BKN, 20.0% CsCl |
| HCEsub-2519-22W | 50.0% BKN, 50.0% CsCl |
| HCEsub-2519-22Z | 36.4% BKN, 63.6% CsCl |
| HCEsub-2519-22B | 83.3% BKN, 16.7% KCl |
| HCEsub-2519-22E | 66.7% BKN, 33.3% KCl |
| HCEsub-2519-22G | 50.0% BKN, 50.0% KCl |

Thermochemical calculations {Table 8} were also conducted on potential HCE smoke replacement formulations based on a blend of BKN igniter with potassium nitrate {KN} and ammonium chloride, ACl. As opposed to KCl and CsCl which are inert, ACl is actually a fuel. Addition of ACl to BKN increases the equivalence ratio {fuel to oxidizer ratio} of the overall formulation. Under these fuel rich conditions, significant quantities of hydrogen chloride are predicted even when the combustion products are allowed in the model to cool to 25 °C. Thus, the thermochemical model suggests that using BKN to vaporize ACl to form an obscurant is not acceptable due to the fact that the right hand side of the following equilibrium becomes more favorable at elevated temperature:

$$NH_4Cl \rightleftharpoons NH_3 + HCl$$

The only acceptable way to incorporate the ACl into a BKN based obscurant formulation is to add additional oxidizer to combust the ammonium. In the calculations summarized in Table 8, the auxiliary oxidizer is potassium nitrate {KN}. Addition of KN to the formulations decreases HCl levels present after the combustion products are cooled to ambient temperature. Formulation development is more complicated in this system relative to BKN/KCl or BKN/CsCl.

**Table 8: Thermochemical modeling of the BKN/$NH_4Cl$/KN obscurant family**

| HCEsub ID | $NH_4Cl$/ KN/BKN Ratio | NASA-Lewis Equiv. Ratio | Flame Temp. @ 1 atm (K) | Flame Temp. @ 1 atm w/ 2X air (K) | FT-FT w/ 2X air (K) | Gas Fraction | Wt Fraction at Flame Temp. | | | | Mass Fraction at 25 C of 2 parts air to 1 part Composition | | | | | | | | |
|---|---|---|---|---|---|---|---|---|---|---|---|---|---|---|---|---|---|---|---|
| | | | | | | | KCl (G) | $K_2CL_2$ (G) | HCl (G) | $B_2O_3$ (L) | KCl | $H_2O$ | $Cl_2$ | $NH_4Cl$ | HCl | $H_3B_3O_6$ | $K_2B_8O_{13}$ | $K_2B_4O_7$ | $K_2CO_3$ |
| BKN | 0/0/10 | 1.81 | 2509 | 2432 | 77 | 0.87 | 0.00 | 0.00 | 0.000 | 0.00 | 0.000 | 0.012 | 0.000 | 0.000 | 0.00000 | 0.000 | 0.188 | 0.159 | 0.000 |
| 2519-22J | 2.5/0/10 | 2.01 | 2146 | 2374 | -228 | 0.87 | 0.08 | 0.00 | 0.027 | 0.00 | 0.101 | 0.035 | 0.000 | 0.001 | 0.00239 | 0.127 | 0.156 | 0.000 | 0.000 |
| 2519-22K | 5/0/10 | 2.18 | 1969 | 2050 | -81 | 0.75 | 0.23 | 0.00 | 0.090 | 0.13 | 0.093 | 0.033 | 0.000 | 0.073 | 0.00221 | 0.118 | 0.145 | 0.000 | 0.000 |
| 2519-22P | 2.5/3.4/10 | 1.48 | 2080 | 2134 | -54 | 0.98 | 0.14 | 0.00 | 0.021 | 0.00 | 0.097 | 0.057 | 0.000 | 0.000 | 0.00000 | 0.000 | 0.226 | 0.047 | 0.000 |
| 2519-22Q | 5.0/5.0/10 | 1.47 | 1981 | 2009 | -28 | 0.89 | 0.17 | 0.00 | 0.068 | 0.11 | 0.068 | 0.198 | 0.011 | 0.000 | 0.00002 | 0.001 | 0.024 | 0.000 | 0.000 |
| 2519-22R | 2.5/6.0/10 | 1.24 | 2329 | 1939 | 390 | 1.00 | 0.08 | 0.00 | 0.037 | 0.00 | 0.090 | 0.053 | 0.000 | 0.000 | 0.00000 | 0.000 | 0.086 | 0.200 | 0.000 |
| 2519-22S | 5.0/8.0/10 | 1.24 | 1920 | 1808 | 112 | 1.00 | 0.12 | 0.00 | 0.079 | 0.00 | 0.162 | 0.086 | 0.000 | 0.000 | 0.00000 | 0.000 | 0.194 | 0.033 | 0.000 |
| 2519-22L | 2.5/10.3/10 | 0.99 | 2519 | 1701 | 818 | 1.00 | 0.07 | 0.00 | 0.029 | 0.00 | 0.081 | 0.048 | 0.000 | 0.000 | 0.00000 | 0.000 | 0.000 | 0.277 | 0.040 |
| 2519-22M | 5/13.1/10 | 1.00 | 2194 | 1608 | 586 | 1.00 | 0.13 | 0.00 | 0.051 | 0.00 | 0.145 | 0.077 | 0.000 | 0.000 | 0.00000 | 0.000 | 0.000 | 0.246 | 0.008 |
| 2519-22N | 7.5/16.0/10 | 0.99 | 1924 | 1557 | 367 | 1.00 | 0.17 | 0.00 | 0.065 | 0.00 | 0.195 | 0.101 | 0.000 | 0.000 | 0.00000 | 0.000 | 0.043 | 0.168 | 0.000 |
| 2519-22O | 10.0/18.8/10 | 1.00 | 1726 | 1535 | 191 | 1.00 | 0.19 | 0.01 | 0.072 | 0.00 | 0.237 | 0.121 | 0.000 | 0.000 | 0.00000 | 0.000 | 0.099 | 0.077 | 0.000 |

Two parameters sets were varied in this modeling study:

1. Maintain the equivalence ratio and vary the ratio of {ACl + KN} to BKN ratio **{different field shading}.** As {ACl + KN} to BKN increases-
    a. The flame temperature decreases as well as the flame temperature resulting from the reaction of the composition with two weight equivalents {thermobaric flame temperature}.
    b. The weight fraction of HCl predicted at flame temperature increases.
    c. The mass fraction of potassium rich borates decreases in the ambient temperature combustion products.
2. Maintain the ACl/BKN ratio and vary KN levels causing variation in the equivalence ratio **{different font colors}.** As KN to ACl/BKN increases-
    a. The thermobaric flame temperature decreases.
    b. Predicted levels of HCl in ambient temperature combustion products decreases.
    c. The mass fraction of potassium rich and increasingly hygroscopic oxides in the ambient temperature combustion products increases.

Formulations selected for experimental evaluation are listed in Table 9. They include two formulations held at an equivalence ratio of 1.00, HCEsub-2519-22M and -22O. HCEsub-2519-22O has a higher ACl/KN to BKN ratio. HCEsub-2519-22P is fuel rich and has low ACl levels. Although fuel rich compositions tend to produce more HCl, formulations with low ACl produce less HCl at flame temperature.

**Table 9: BKN/ACl/KN formulations selected for performance evaluation**

| ID | Formulation | Equivalence Ratio |
|---|---|---|
| HCEsub-2519-22P | 62.9 % UIX-156, 15.72% ACl, 21.38% KN | 1.48 |
| HCEsub-2519-22M | 35.59 % UIX-156, 17.79% ACl, 46.62% KN | 1.00 |
| HCEsub-2519-22O | 25.77% UIX-156, 25.77% ACl, 48.46 % KN | 1.00 |

### 5.2.2 Ingredient Compatibilities

Ingredient compatibilities were conducted on ingredients in the hexachloroethane baseline obscurant (18) and the blends of BKN with halide salts (19). Data are summarized in Table 10. VTS was conducted on the BKN/ACl ingredient pair. Minimal gas evolution was expected from the other ingredient pairs. No incompatibilities were identified below 200 °C. New exotherms were identified for ingredient pairs BKN/CsCl {Figure 18} and BKN/$NH_4Cl$ {Figure 19}.

**Table 10: Compatibility data for HCE baseline ingredients and BKN with halide salts.**

| Ingredient A | Ingredient B | DSC onset {$^oC$} | VTS {mL/g} |
|---|---|---|---|
| BKN | KCl | None from 25 – 350 | NR* |
| BKN | CsCl | 241 °C | NR |
| BKN | ACl | 215 °C | -0.018 |
| Hexachloroethane | Zinc Oxide | None from 25 – 350 | NR |
| Hexachloroethane | Aluminum | “ | NR |
| Zinc Oxide | Aluminum | “ | NR |
| Hexachloroethane | ZnO/Al | “ | NR |

*NR = Not Required

Thermal compatibility data **(20)** were acquired for obscurant formulations tested in the 100 cubic foot chamber and the urethane adhesive used to attach their respective pellets to roofing nails {Figure 9}. The data are summarized in Table 11. The VTS for “22M” produced slightly more gas than typically allowed, 2.0 ml/g. However this test was run at 120 °C. If it had been ran at 100 °C, it would most likely pass the test which is still >100 °F above handling temperature.

**Table 11: Compatibility data for D50 Urethane adhesive with obscurant formulations**

| Ingredient A | Ingredient B | DSC onset {$^oC$} | VTS {mL/g} |
|---|---|---|---|
| HCEsub-2519-22M | D50 Urethane | None from 25 – 350 | 2.1* |
| HCE-1691-68A | D50 Urethane | “ | 1.0 |
| HCEsub-2519-22Z | D50 Urethane | “ | 1.4 |
| HCEsub-2519-22G | D50 Urethane | Chemically Similar to “22Z” | |

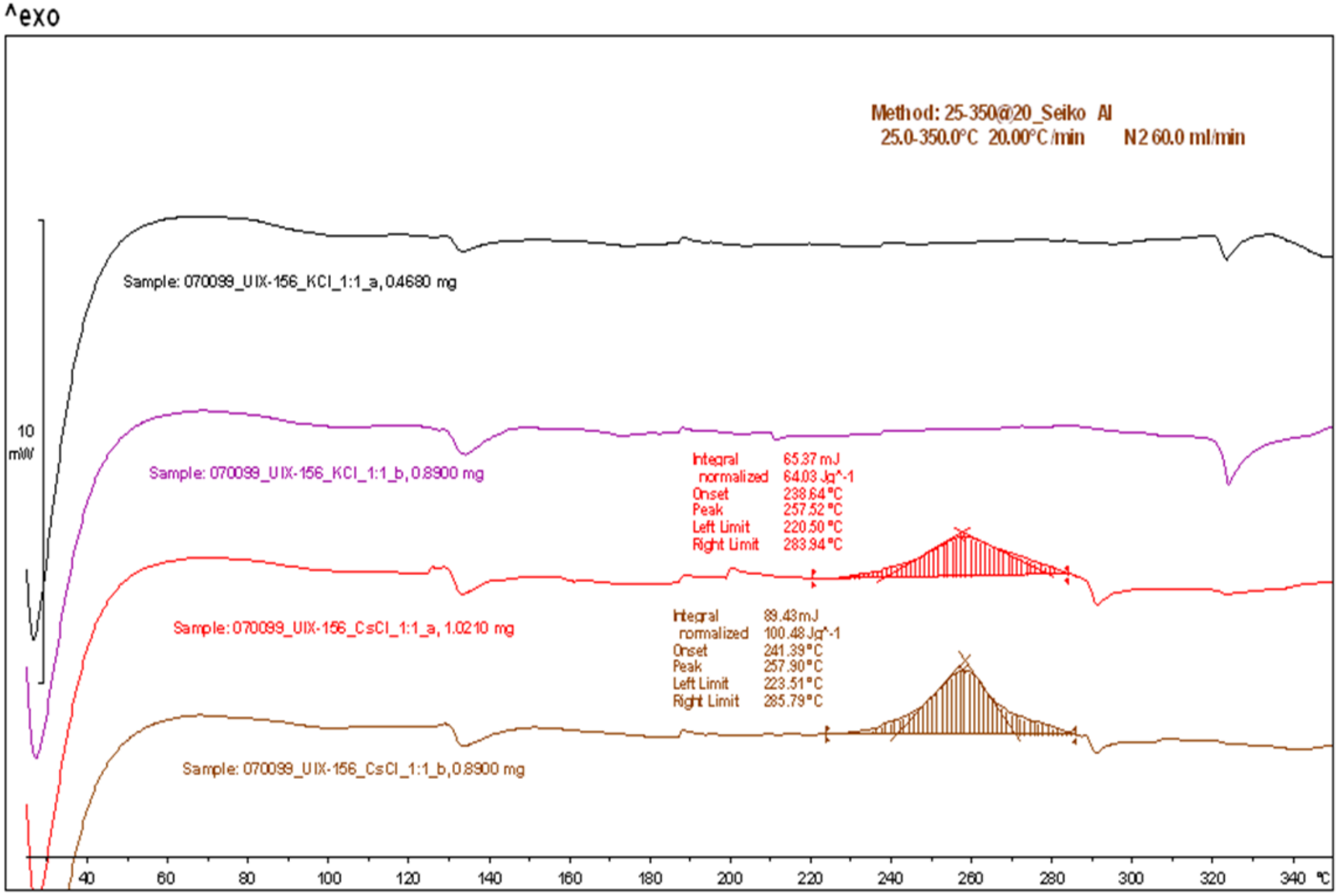


**Figure 18: DSC Thermograms for BKN {UIX-156}/KCl {black and violet traces} and BKN/CsCl {red and brown traces}. The bar along the y-axis is equivalent to 10 mW. Exothermic peaks are positive relative to baseline.**

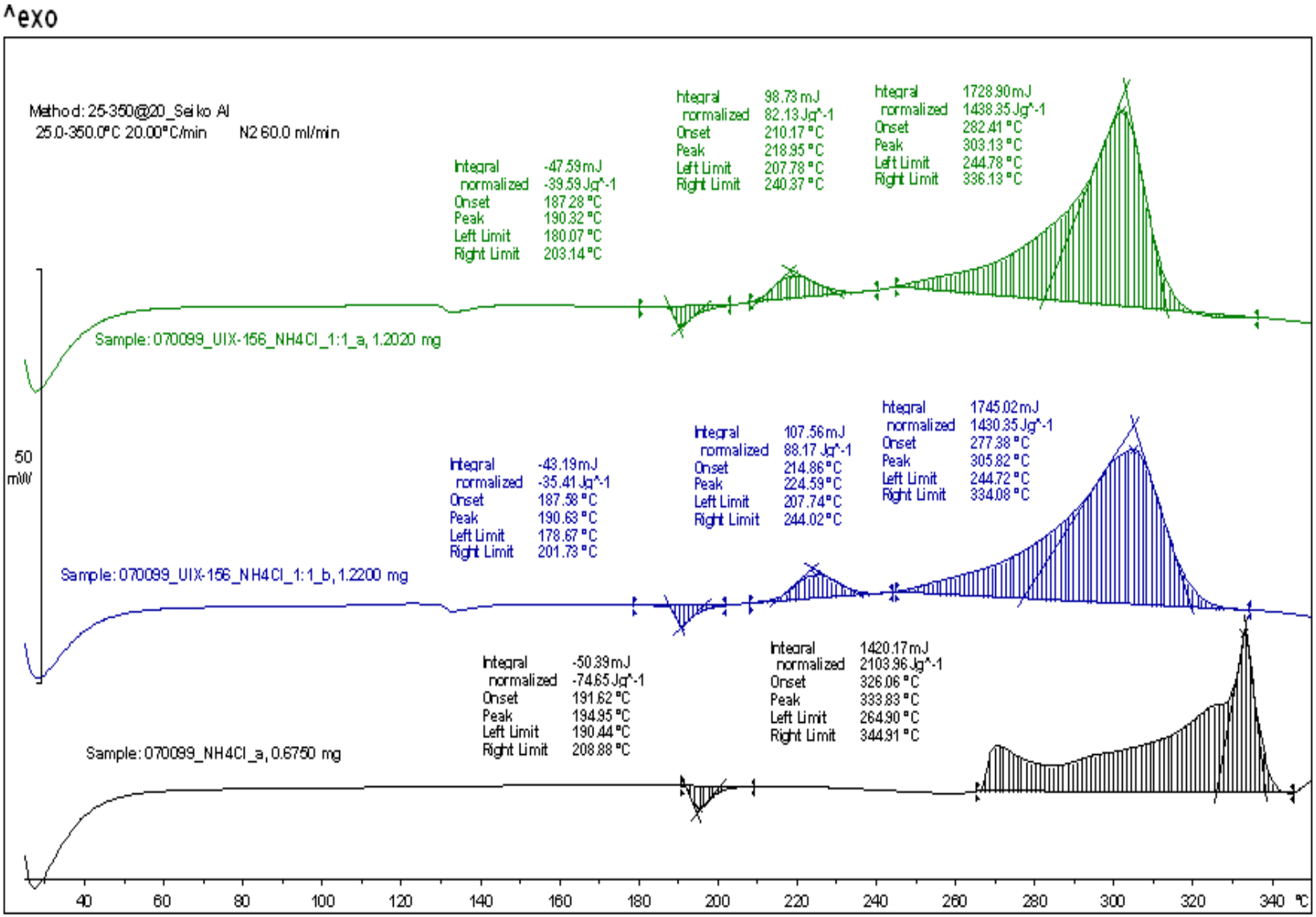


**Figure 19: DSC Thermograms for BKN/ACl {green and blue traces} and neat ACl {black trace}. The bar along the y-axis is equivalent to 50 mW. Exothermic peaks are positive relative to baseline.**

### 5.2.3 **Hazard Sensitivity**

Hazard sensitivity data for the hexachloroethane baseline obscurant and the obscurant candidates containing BKN blended with halide salts are summarized in Table 12. In many cases, only limit testing {Section 5.5} was conducted to determine that the formulations were acceptable for handling according to company safety standards {AHOPS}. Formulations deemed intermediate in reactivity within a family were not tested for hazard sensitivity.

The baseline test formulation selected for these studies is the following:

| | |
|---|---|
| Aluminum, MIL-A-512A, Type II, Grade C, Class 4 | 9.0 pbw |
| Hexachloroethane, MIL-H-235 | 44.5 pbw |
| Zinc Oxide, MIL-Z-291C, Grade A, Class 1 | 46.5 pbw |

### 5.2.4 **Initial Formulation Screening**

Consolidated samples of the baseline formulation and replacement BKN/halide salt candidates were ignited in a fume hood approved for burning small samples of pyrotechnics and other energetic materials {Section 5.7}. This was used as a qualitative means of down selecting the most promising candidates:

1. Formulations containing -60 mesh boron/potassium nitrate granulated igniter composition dry blended in the Speed Mixer {Section 5.4} with selected chloride salts showed more promise than silicon based formulations {Section 6.1.4} when pellets thereof were ignited in the hood. Samples of the boron/potassium nitrate burned less rapidly as greater portions of the halide salt were blended therein.
    a. Compositions with ammonium chloride, 22M, 22O and 22P, were also blended with potassium nitrate to ensure complete combustion of the ammonium ion. The composition, 22O, produced large amounts of slag and was eliminated from further consideration. 22M combusted more slowly than 22P and was selected for initial testing in the test chamber.
    b. Compositions with potassium chloride, 22B, 22E and 22G, produced significant quantities of smoke. 22B burned very rapidly and was eliminated from further consideration. 22G combusted more slowly than 22E and was selected for initial testing in the chamber.
    c. Compositions with cesium chloride, 22T, 22W and 22Z, produced significant quantities of smoke. 22Z combusted most slowly and appeared to produce the most amount of smoke. It was selected for initial testing in the chamber. It is noteworthy, that 22Z is significantly denser than the other compositions allowing loading of a greater mass of obscurant in a volume constrained grenade.

The baseline HCE obscurant was significantly more difficult to ignite than the BKN based obscurant candidates. Once ignited, it did produce copious amounts of smoke when tested in the hood.

**Table 12: Hazard sensitivity data for the hexachloroethane baseline obscurant and the obscurant candidates containing BKN blended with halide salts**

| Material | STR Number | ABL ESD | Bulk ESD | ABL Friction | Impact | Autoignition {SBAT} |
|---|---|---|---|---|---|---|
| AHOPS Requirements | NA | > 0.075 J | NA | > 40 lbs @ 1 ft/sec | >7 cm {ABL} | >225 F |
| HCE Obscurant Baseline | 31122 | 5.656 | NA | 320 lbs @ 8 ft/sec | 64 | >500 ºF, no reaction, no burn |
| HCEsub-2519-22T 80% BKN, 20% CsCl | 31119 | > 0.075 J | NA | >40 lbs @ 3 ft/sec | >6.9 cm | 415 ºF, exotherm, no burn |
| HCEsub-2519-22W 50% BKN, 50% CsCl | NA | Interpo-lation | Interpo-lation | Interpo-lation | Interpo-lation | Interpolation. |
| HCEsub-2519-22Z 36.36% BKN, 63.64% CsCl | 31120 | > 0.075 J | NA | >40 lbs @ 3 ft/sec | >6.9 cm | 427 ºF, exotherm, no burn |
| HCEsub-2519-22B 83.33% BKN, 16.67% KCl | 31117 | > 0.075 J | NA | >40 lbs @ 3 ft/sec | >6.9 cm | 402 ºF, exotherm, no burn |
| HCEsub-2519-22E 66.67% BKN, 33.33% KCl | NA | Interpo-lation | Interpo-lation | Interpo-lation | Interpo-lation | Interpolation. |
| HCEsub-2519-22G 50% BKN, 50% KCl | 31118 | 5.656 J | NA | 560 lbs @ 8 ft/sec | 80 cm | 430 ºF, exotherm, no burn |
| HCEsub-2519-22P 62.9 % BKN, 15.72% ACl, 21.38% KN | | > 0.075 J | NA | >40 lbs @ 3 ft/sec | >6.9 cm | 313 F, Exotherm, Burned |
| HCEsub-2519-22M 35.59 % BKN, 17.79% ACl, 46.62% KN | NA | Interpo-lation | Interpo-lation | Interpo-lation | Interpo-lation | Interpolation. |
| HCEsub-2519-22O 25.77% BKN, 25.77% ACl, 48.46 % KN | | > 0.075 J | NA | >40 lbs @ 3 ft/sec | >6.9 cm | 311 F, Exotherm, Burned |

### 5.2.5 **Pellet Density Measurements**

Pellets were pressed according to the method in Section 5.6. Pellet density data are summarized in Table 13. The baseline pellets have the largest density. This is significant because a larger mass of this obscurant can be housed in the volume-limited payload compartment of a smoke grenade. The 22Z formulation of BKN/CsCl has a slightly lower density whereas the BKN/KCl and BKN/ACl formulations have significantly lower densities. From this data alone, 22Z would be the most favored obscurant replacement formulation because of its favorable density.

**Table 13: Comparison of obscurant pellet densities**

| ID | Formulation | Number of Pellets Measured | Pellet Density (g/cc) | |
|---|---|---|---|---|
| | | | Average | Standard Deviation |
| HCE | HCE | 10 | 2.42 | 0.04 |
| 22G | BKN/KCl | 8 | 1.40 | 0.02 |
| 22M | BKN/ACl | 7 | 1.50 | 0.01 |
| 22Z | BKN/CsCl | 7 | 2.28 | 0.09 |

### 5.2.6 **Hundred Cubic Foot Chamber Transmittance Analysis at ATK**

Pellets of the hexachloroethane obscurant baseline and HCE obscurant replacement formulations, HCEsub-2519-22G {BKN/KCl}, -22M {BKN/ACl} and -22Z {BKN/CsCl} were tested in the ATK 100 cubic foot test chamber according to the method described in Section 5.8 to obtain transmittance data. The data are summarized in tabulated form in Table 14. During testing, it was observed that pellet #1 of the HCE baseline quenched before combustion was complete. When the baseline $-\log_{10}$transmittance data are divided by pellet height, they become normalized according to packing efficiency in a cylindrical volume. The transmittance for pellet #1 is significantly higher than expected relative to transmittance measurements obtained for the other pellets. Thus, the value for pellet #1 is not included in the plot of $-\log_{10}$transmittance vs. pellet weight in Figure 20.

The data suggest that the $-\log_{10}$ of transmittance are roughly proportional to pellet weight for the HCE baseline composition as tested in the 100 cubic foot chamber. A plot through the one-gram and two-gram data have a steeper slope than a plot through the one-gram and three-gram data. When pellet #1 data are excluded, transmittance data normalized for packing efficiency show a steady decrease therein with increasing pellet height. Additional data would need to be acquired to determine if this decrease in obscurant efficiency as a function of sample weight is real. It could be due to a greater amount of particle settling or adhesion to the chamber walls with the increased particulate concentration in the chamber.

Unfortunately, the $-\log_{10}$ transmittance values for the selected BKN based obscurant candidates are a quarter of those obtained for pellets of the baseline formulation of equivalent mass of three grams. Of the three BKN formulations, efficiency increases as follows: BKN/ACl < BKN/CsCl < BKN/KCl. If the data are normalized for packing efficiency, BKN/CsCl is almost twice as efficient as the formulations with KCl and ACl but still only a quarter as efficient as the baseline. When testing these samples in the ATK 100 cubic foot chamber, it was noticed that a considerable amount of slag was produced when these pellets were combusted. This suggests that a considerable amount of solid combustion products were not converted to smoke and that

obscurant efficiency would increase if halide salt were removed from these formulations. This would increase the flame temperature and promote the evolution of more smoke improving obscurant efficiency. These BKN rich formulations would have burn rates significantly higher than that of the HCE baseline formulation. Higher levels of BKN in BKN/CsCl will decrease its packing efficiency. However, if more of the combusted solids form an aerosol instead of slag, transmittance per unit volume of obscurant should still increase significantly.

**Table 14: Transmittance data**

| ID | pellet # | Pellet Weight (g) | pellet height (in) | Transmittance | -Log Transmittance | -log Transmittance/ pellet height |
|---|---|---|---|---|---|---|
| HCE-1g | 2 | 1.05 | 0.1325 | 0.417 | 0.3794 | 2.86 |
| | 1 | 1.05 | 0.1385 | 0.567 | 0.2461 | 1.78 |
| Ave-1g | | | | 0.492 | 0.313 | 2.32 |
| Std Dev-1g | | | | 0.106 | 0.094 | 0.77 |
| HCE-2g | 3 | 2.03 | 0.2630 | 0.213 | 0.6707 | 2.55 |
| | 4 | 2.04 | 0.2615 | 0.201 | 0.6959 | 2.66 |
| Ave-2g | | | | 0.207 | 0.683 | 2.61 |
| Std Dev-2g | | | | 0.008 | 0.018 | 0.08 |
| HCE-3g | 8 | 3.01 | 0.3875 | 0.138 | 0.8594 | 2.22 |
| | 9 | 3.01 | 0.3975 | 0.159 | 0.7977 | 2.01 |
| Ave-3g | | | | 0.149 | 0.829 | 2.11 |
| Std Dev-3g | | | | 0.015 | 0.044 | 0.15 |
| 22G (BKN/ KCl)-3g | 16 | 2.99 | 0.6585 | 0.577 | 0.2390 | 0.36 |
| | 17 | 3.00 | 0.6650 | 0.579 | 0.2377 | 0.36 |
| | 18 | 3.01 | 0.6610 | 0.612 | 0.2129 | 0.32 |
| | 19 | 3.00 | 0.6630 | 0.579 | 0.2374 | 0.36 |
| Ave-3g | | | | 0.587 | 0.232 | 0.35 |
| Std Dev-3g | | | | 0.017 | 0.013 | 0.02 |
| 22M (BKN/ ACl)-3g | 20 | 3.00 | 0.6155 | 0.631 | 0.2001 | 0.33 |
| | 21 | 3.01 | 0.6140 | 0.670 | 0.1739 | 0.28 |
| | 22 | 3.01 | 0.6230 | 0.631 | 0.1997 | 0.32 |
| Ave-3g | | | | 0.644 | 0.191 | 0.31 |
| Std Dev-3g | | | | 0.022 | 0.015 | 0.02 |
| 22Z (BKN/ CsCl)-3g | 12 | 3.01 | 0.3900 | 0.606 | 0.2177 | 0.56 |
| | 13 | 3.01 | 0.3970 | 0.579 | 0.2375 | 0.60 |
| | 14 | 3.02 | 0.4000 | 0.609 | 0.2157 | 0.54 |
| Ave-3g | | | | 0.598 | 0.224 | 0.57 |
| Std Dev-3g | | | | 0.016 | 0.012 | 0.03 |

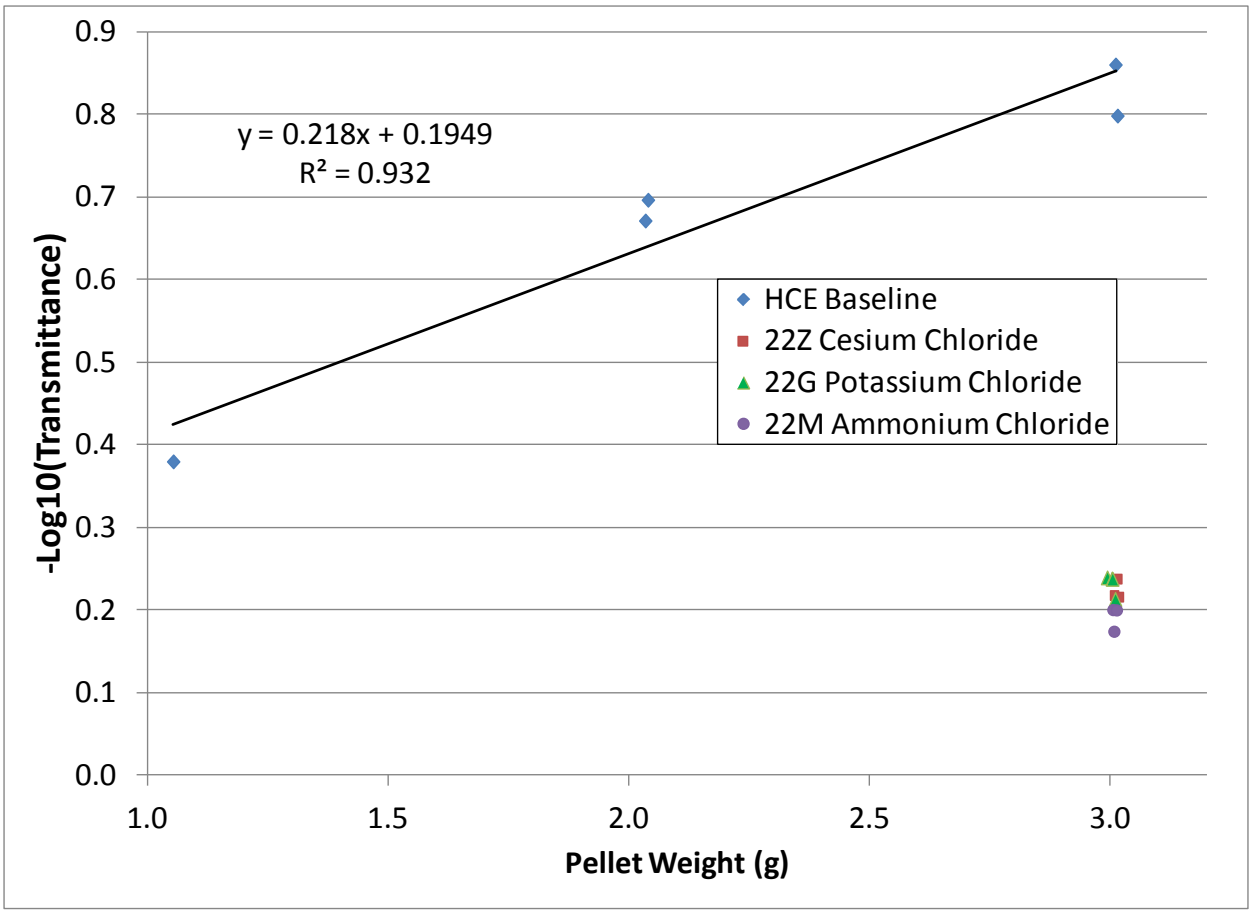


**Figure 20: Comparison of HCE baseline transmittance with that of the BKN based obscurant candidates**

### 5.2.7 Hundred Cubic Foot Chamber Particulate Analysis at Autoliv

Particulate data were collected in an Autoliv 100 cubic foot test chamber {Figure 12} on three-gram pellets only. Total particulate data are summarized in Table 15. Particulate data as a function of particle size are tabulated in Table 16. Particle size data were collected in duplicate for each formulation. Averaged values are plotted in Figure 21.

Total particulate concentration is significantly higher for the baseline formulation than for the BKN formulations. This is consistent with the higher $-\log_{10}$transmittance observed for the baseline formulation.

**Table 15: Autoliv total particulate data**

| ID | pellet # | Total Particulate-Filter ($mg/m^3$) | Total Particulate-Anderson ($mg/m^3$) | Percent Decrease in Anderson relative to Filter Data |
|---|---|---|---|---|
| HCE | 36 | 471 | 441 | 6 |
| | 37 | 526 | 467 | 11 |
| Ave | | 499 | 454 | 9 |
| Std Dev | | 39 | 18 | 3 |
| 22G | 28 | 98 | 81 | 17 |
| (BKN/KCl) | 29 | 79 | 72 | 9 |
| Ave | | 89 | 77 | 13 |
| Std Dev | | 13 | 6 | 6 |
| 22M | 33 | 115 | 86 | 25 |
| (BKN/ACl) | 34 | 116 | 78 | 33 |
| Ave | | 116 | 82 | 29 |
| Std Dev | | 1 | 6 | 5 |
| 22Z | 24 | 222 | 226 | -2 |
| (BKN/CsCl) | 25 | 181 | 178 | 2 |
| Ave | | 202 | 202 | 0 |
| Std Dev | | 29 | 34 | 2 |

**Table 16: Anderson impactor particulate values**

| **Formulation ID** | 22Z | | 22G | | 22M | | HCE | |
|---|---|---|---|---|---|---|---|---|
| **Formulation** | BKN/CsCl | | BKN/KCl | | BKN/ACl | | Baseline | |
| **Pellet Number** | 24 | 25 | 28 | 29 | 33 | 34 | 36 | 37 |
| **Particulate Concentrations (microns)** | | | | | | | | |
| 3.3 - 4.7 | 3 | 3 | 1 | 1 | 2 | 1 | 1 | 3 |
| 2.1 - 3.3 | 19 | 13 | 1 | 3 | 1 | 1 | 7 | 9 |
| 1.1 - 2.1 | 123 | 120 | 29 | 29 | 11 | 16 | 366 | 370 |
| 0.7 - 1.1 | 60 | 30 | 35 | 27 | 29 | 26 | 58 | 69 |
| 0.4 - 0.7 | 10 | 8 | 11 | 9 | 30 | 24 | 9 | 15 |
| < 0.4 | 11 | 4 | 4 | 3 | 13 | 10 | 0 | 1 |
| Total | 226 | 178 | 81 | 72 | 86 | 78 | 441 | 467 |

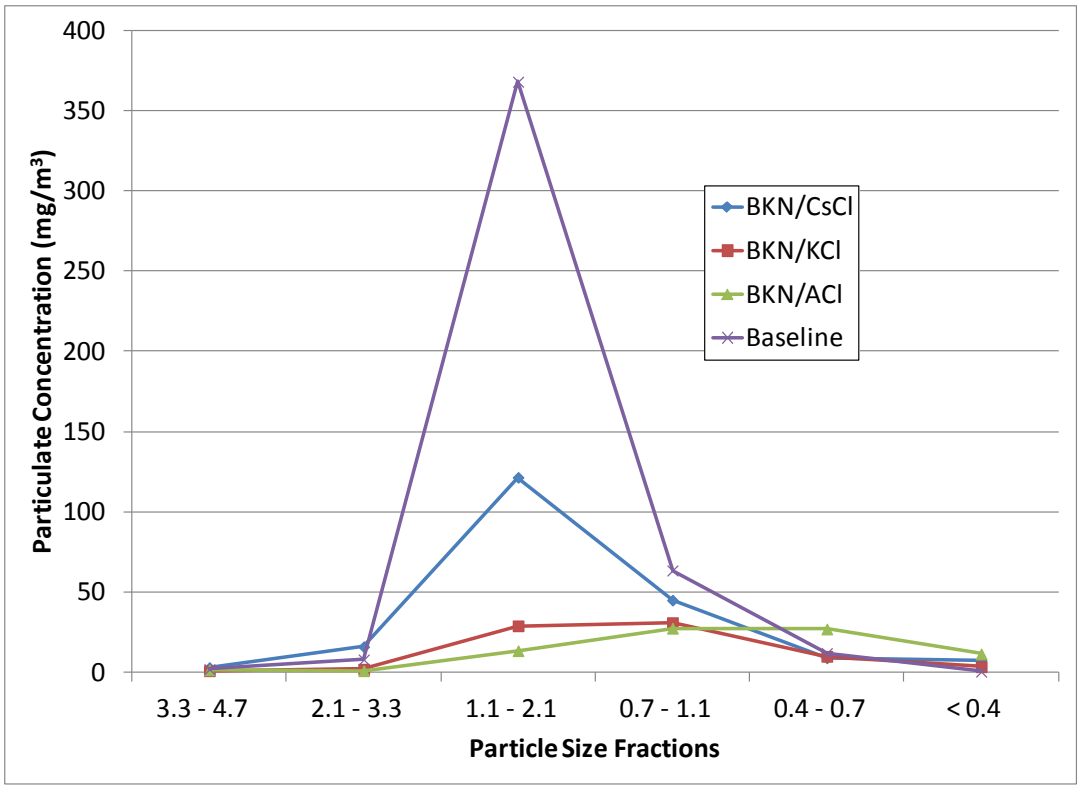


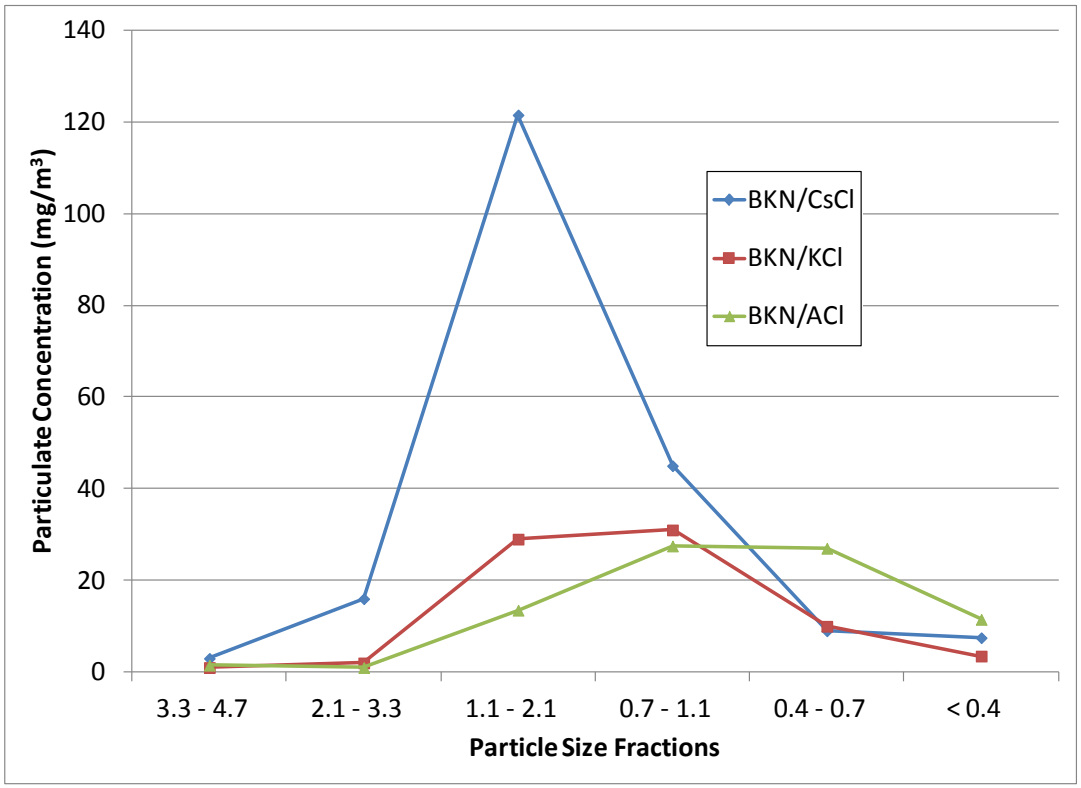


**Figure 21: Average Anderson impactor data: top-all data, bottom-BKN formulations**

The particulate mass per unit volume for BKN/CsCl in Table 15 is significantly higher than for BKN/KCl and BKN/ACl even though $-\log_{10}$transmittance values are comparable. Obscurant performance is more a function the number of particles per unit volume whereas the particulate

concentration reported in Tables 15 and 16 is a function particulate mass per unit volume. The BKN/CsCl particles contain significant amounts of cesium. The presence of cesium in the particles will increase particle density. Assuming comparable particle populations due to near equal transmittance values, it is logical that the total mass of the BKN/CsCl particles in a given volume will be higher than that for BKN/KCl and BKN/ACl. If the same volume of BKN/CsCl was tested as BKN/KCl or BKN/ACl, $-\log_{10}$transmittance values for the BKN/CsCl are predicted to be, by far, the highest since the total weight of the more dense BKN/CsCl sample would be higher.

The Anderson impactor values for total particulate in Table 15 are lower than total particulate values collected on a filter {See Section 5.9.4}. Chris Erickson of Autoliv stated that collection of particulates on the Anderson Impactor started ten minutes later than collection of total particulates (13). He stated that the lower values obtained from the impactor were most likely due to particulate settling or adhesion to the chamber surface during the ten minutes before impactor data was collected. The percent decrease in "Anderson" relative to "filter" total particulates in Table 16 trends as follows:

BKN/CsCl < BKN/KCl < BKN/ACl

The average particulate size {See Table 16 and Figure 21} decreases as the difference in "Anderson" and "filter" values increase:

BKN/CsCl > BKN/KCl > BKN/ACl

It seems counterintuitive that smaller particles would settle out more readily than larger particles. Transmittance values appear to be relatively stable once mixing of the particulates in the 100 cubic foot chamber is complete {See Figure 10}.

The percentage of condensable gases produced in the combustion products; e.g., nitrogen, water and carbon dioxide; increases as the particle size decreases:

BKN/CsCl {8.0% total, 1.3% $H_2O$} < BKN/KCl {11.6%, 1.8%} < BKN/ACl {32.6%, 15.5%}

Possibly, the gas produced upon combustion promotes formation of a finer aerosol. Solids in silica based obscurant formulations discussed in Section 6.1 produced aerosols more efficiently when more non-condensible gases were produced upon combustion.

It is also possible that water becomes entrained in the particulates of the aerosol during combustion and evaporates out of the particles during the first ten minutes in the test chamber. This would also cause a decrease in the particulate mass per unit volume for "Anderson" values relative to "filter" values. The following data are supportive of this premise: BKN/ACl produces by far the most amount of water upon combustion, 15.5% vs. 1.8% for BKN/KCl. Its particulate concentration is significantly higher than BKN/KCl when measured for total particulates by the "filter" method, 116 vs. 89 $mg/m^3$, whereas it's particulate concentration by the "Anderson" method is comparable to that of BKN/KCl, 82 vs. 77 $mg/m^3$. Possibly, water entrained in the particulate vaporizes in the ten minutes before "Anderson" testing began.

### 5.2.8 **Toxic Gas Analysis**

Methodology is summarized in Sections 5.8 and 5.9.2. All toxic gas analysis results, both from ATK and Autoliv, are summarized in Table 17. Values in red were collected at Autoliv using the FT-IR spectrometer. Where cells are left blank, a measurement was not taken. In some cases, gases were monitored but were below or above the detection limit. Gases that were monitored by FT-IR but not detected that are not listed in Table 17 are listed in Table 18.

Hydrogen chloride values were monitored using HCl Draeger tubes. The HCE baseline hydrogen chloride values are roughly proportional to pellet weight {Figure 22}. The values for the baseline measured for three-gram pellets are barely below the OSHA PEL ceiling for hydrogen chloride of 5 ppm. Hydrogen chloride is also detected in the gaseous combustion products for BKN/Halide salt compositions. The levels are significantly lower for BKN/CsCl and BKN/KCl than for the HCE baseline composition at the three-gram obscurant sample size.

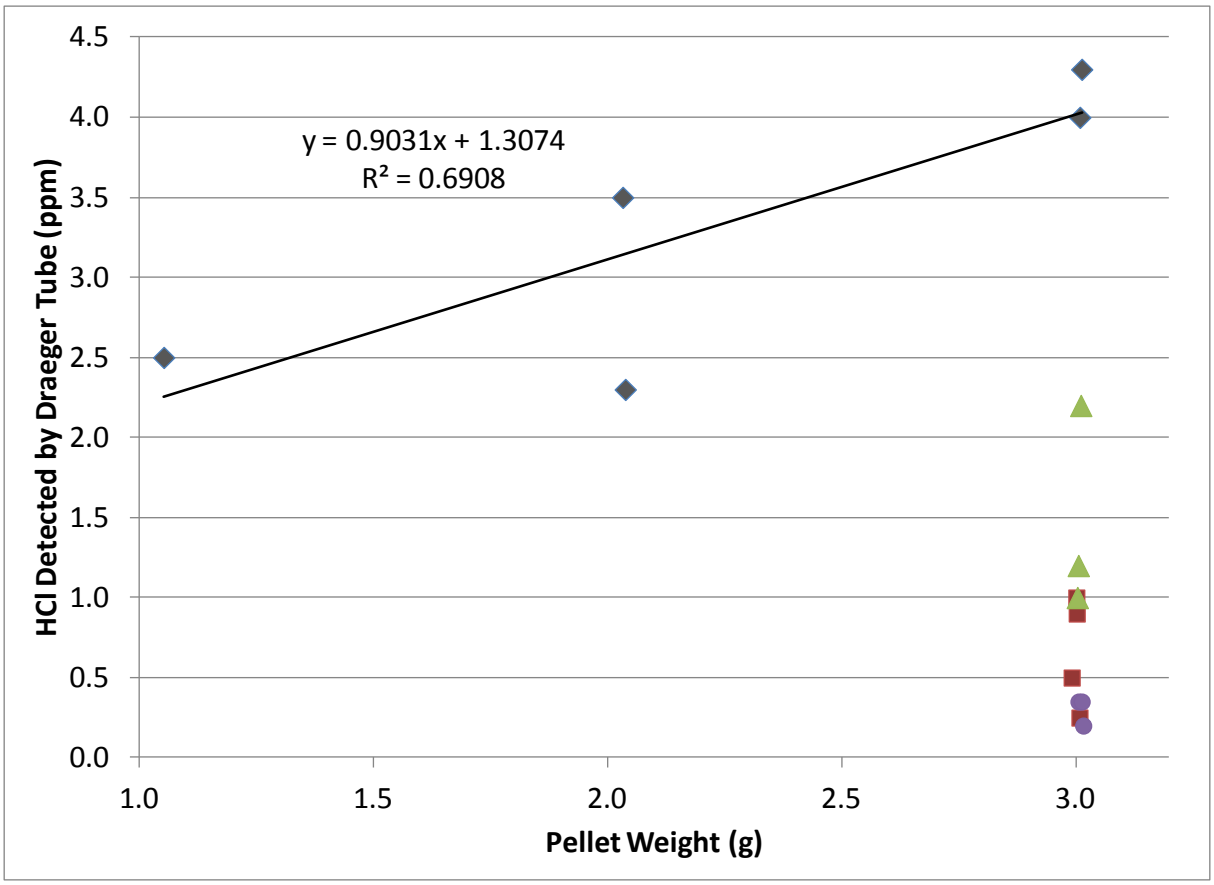


**Figure 22: Hydrogen chloride levels plotted as a function of obscurant sample weight**

**Table 17: Toxic gas analysis data**

| ID | pellet # | Hydrogen Chloride by HCl 0.2/a Draeger Tube or FT-IR (ppm) | Phosgene by Draeger CMS or FT-IR (ppm) | Carbon Dioxide, FT-IR (ppm) | Carbon Monoxide by CO 10/b Draeger Tube or FT-IR (ppm) | Nitrous Gases, 20/a Draeger Tube (ppm) | Nitric Oxide, FT-IR (ppm) | Nitrogen Dioxide, FT-IR (ppm) |
|---|---|---|---|---|---|---|---|---|
| OSHA PEL (ppm) | | 5 | 0.1 | 5000 | 50 | | 25 | 5.0 |
| HCE-1g | 2 | 2.5 | NM | | | | | |
| | 1 | 0.7 | | | | | | |
| HCE-2g | 3 | 3.5 | 0.77 | | 18 | | | |
| | 4 | 2.3 | | | | << 20 | | |
| HCE-3g | 8 | 4.0 | 0.62 | | | | | |
| | 9 | 4.3 | >2 | | | | | |
| | 36 | <2.6 | <0.9 | 405 | <17 | | <0.9 | <0.9 |
| | 37 | <2.6 | <0.9 | 418 | 22 | | <0.9 | <0.9 |
| 22G (BKN/ KCl)-3g | 16 | 0.5 | | | | 20 | | |
| | 17 | 1.0 | | | | 20 | | |
| | 18 | 0.3 | | | 5 | | | |
| | 19 | 0.9 | | | 7 | 20 | | |
| | 28 | <2.6 | <0.9 | 433 | <17 | | 16 | <0.9 |
| | 29 | <2.6 | <0.9 | 402 | <17 | | 14 | <0.9 |
| 22M (BKN/ ACl)-3g | 20 | 1.0 | | | | 65 | | |
| | 21 | 1.2 | | | <<10 | 70 | | |
| | 22 | 2.2 | | | 2 | 50 | | |
| | 32 | <2.6 | | 435 | <17 | | 39 | 6.5 |
| | 33 | <2.6 | <0.9 | 531 | <17 | | 37 | 5.1 |
| | 34 | <2.6 | <0.9 | 414 | <17 | | 37 | 5.4 |
| 22Z (BKN/ CsCl)-3g | 12 | 0.4 | | | | 15 | | |
| | 13 | 0.4 | | | 10 | 17 | | |
| | 14 | 0.2 | | | 7 | | | |
| | 24 | <2.6 | <0.9 | 393 | <17 | | 13 | <0.9 |
| | 25 | <2.6 | <0.9 | 381 | <17 | | 11 | <0.9 |

**Table 18: Additional toxic gases measured but not detected**

| Toxic Gas | Detection Limit (ppm) |
|---|---|
| Hydrogen Cyanide | <1.7 |
| Ammonia | <0.9 |
| Chlorine | <0.2 |
| Acetylene | <0.86 |
| Ethylene | <0.86 |
| Benzene | <2.6 |
| Other Hydrocarbons | <3.1 |
| Ethanol | <1.7 |
| Formaldehyde | <0.86 |
| Sulfur Dioxide | <0.86 |

Both HCE baseline and BKN/halide compositions produce carbon monoxide and carbon dioxide. Carbon dioxide levels are well below PEL limits in all compositions. Carbon monoxide levels are highest in the HCE baseline and lowest in BKN/ACl. This is consistent with the fuel content in the formulations. All of the formulations are fuel rich except for BKN/ACl. The values detected in the HCE baseline are still half of the carbon monoxide PEL value.

The HCE baseline produces phosgene levels well above the PEL limit but produce no nitrous gases. The fuel balanced BKN/ACl produces levels of nitric oxide and nitrogen dioxide slightly higher than the respective OSHA PEL limits. The fuel rich BKN/CsCl and BKN/KCl produce low levels of nitric oxide but no nitrogen dioxide.

In summary, the HCE baseline produces high levels of hydrogen chloride and phosgene but produces no nitrous gases. The BKN/halide salt compositions produce lower levels of hydrogen chloride but do produce nitrous gases especially when they are formulated to have balanced levels of fuel and oxidizer.

### 5.2.9 Chemical Analysis of Respirable Obscurant Particulates

According to test results from the Anderson impactor {Table 16 and Figure 21}, most of the particulate was found to be less than 2.1 μm in size, which is considered respirable. Material on impactor plates representing particulate less than 3.3 μm in size were analyzed for chemical content. Analyses were conducted on water soluble {WS} and water insoluble/acid soluble {WIAS} fractions {See Section 5.9}. A summary of elements and ions of significance identified in the WS and WIAS fractions are summarized in Table 19 as well as an estimate of the amount of the water insoluble/acid insoluble {WIAI} fraction in each type of particulate. Blank values in Table 19 are below the detection limit. Analysis of other ions and elements were conducted but were insignificant or below detectable levels. These entities and their detection limits or highest levels detected are listed in Table 20.

**Table 19: Analysis of elements and ions in obscurant particulates**

| Formulation ID | | 22Z | | 22G | | 22M | | HCE Baseline | |
|---|---|---|---|---|---|---|---|---|---|
| Formulation | | BKN/CsCl | | BKN/KCl | | BKN/ACl | | | |
| Pellet Number | | 24 | 25 | 28 | 29 | 33 | 34 | 36 | 37 |
| Chemical Entity Concentration (mg/m$^3$) | | | | | | | | | |
| Aluminum | WS ICP | | | | | | | 0.51 | 0.44 |
| | WIAS ICP | | | | | | | 1.4 | 1.5 |
| Zinc | WS ICP | | | | | | | 120 | 120 |
| | WIAS ICP | | | | | | | 3.9 | 3.8 |
| Boron | WS ICP | 5.3 | 3.8 | 3.2 | 2.7 | 4.2 | 4 | | |
| | WIAS ICP | 0.35 | 0.45 | 0.06 | 0.11 | 0.09 | 0.1 | | |
| Magnesium | WS ICP | 0.1 | 0.21 | 0.1 | 0.11 | | | | |
| | WIAS ICP | | 0.05 | | | | | | |
| Potassium | WS ICP | 14 | 9.8 | 28 | 23 | 29 | 26 | | |
| | WIAS ICP | 1.7 | 2.1 | 2.3 | 2.5 | 2.3 | 2.7 | | |
| Chloride | WS Anion IC | 27 | 22 | 23 | 19 | 27 | 23 | 169 | 169 |
| Cesium | WS Cation IC | 100 | 78 | | | | | | |
| Calculated Oxygen | | 15.8 | 12.0 | 8.3 | 7.2 | 9.8 | 9.8 | 1.7 | 1.7 |
| Calculated $C_xCl_{2x}O_x$ | | 0.0 | 0.0 | 0.0 | 0.0 | 0.0 | 0.0 | 48.3 | 48.5 |
| Sum WS and WIAS | | 164 | 128 | 65 | 55 | 72 | 66 | 345 | 345 |
| Total Respirable | | 223 | 175 | 80 | 71 | 84 | 77 | 440 | 464 |
| Total WIAI | | 59 | 47 | 15 | 16 | 12 | 11 | 95 | 119 |

**Table 20: Upper possible concentration level of other elements or ions**

| Element or Ion | Detection Limit | Element or Ion | Detection Limit | Element or Ion | Detection Limit |
|---|---|---|---|---|---|
| Aluminum | <0.36 | Lead | <0.057 | Strontium | <0.036 |
| Antimony | <0.043 | Magnesium | <0.064 | Tin | <0.043 |
| Arsenic | <0.043 | Manganese | <0.043 | Titanium | <0.036 |
| Barium | <0.036 | Mercury | <0.7 | Zinc | <0.021 |
| Bismuth | <0.36 | Molybdenum | <0.036 | Zirconium | <0.028 |
| Boron | <0.07 | Nickel | <0.021 | Chloride | 27 |
| Cadmium | <0.028 | Phosphorus | <0.1 | Cyanate | <0.8 |
| Calcium | <0.4 | Potassium | <0.5 | Fluoride | <0.8 |
| Chromium | <0.028 | Selenium | <0.036 | Nitrate | <0.8 |
| Cobalt | <0.028 | Silicon | <0.072 | Nitrite | <0.8 |
| Copper | <0.028 | Silver | <0.05 | Sulfate | <1 |
| Iron | <0.028 | Sodium | <2 | Ammonium | <0.8 |

It is noteworthy that nitrate and ammonium are on the "not detected" list. This suggests that nitrate was almost completely consumed during the combustion of BKN/halide salt formulation. It also suggests that ammonium chloride was almost completely consumed during the combustion of BKN/ACl. This may also account for the fact that the BKN/ACl particulate is so small {Figure 21}. It was not produced due to the volatilization of the chloride salt but through combustion of ACl by KN to produce KCl, nitrogen and water.

By calculating molar ratios of the various elements detected in the respirable particulates, further information can be gleaned from this data {Table 21 and Table 22}. For example, by determining the number of millimoles/$m^3$ of chloride detected in BKN/CsCl, the concentration of cesium accompanying it in cesium chloride can be calculated. The calculated value for cesium in cesium chloride agrees well with the amount analyzed {Table 21}.

The concentration of potassium was calculated necessary to accompany chloride in KCl. In all three BKN/halide salt formulations, residual potassium was left over. This was assigned to combustion products of BKN. From this, the mole ratio of potassium to boron in the BKN combustion products could be assigned {Table 21}. In all three formulations, there is less than one potassium ion present for every ion of boron. The potassium content decreases in the order BKN/CsCl > BKN/KCl > BKN/ACl. The composition for the BKN based particulates produced in BKN/CsCl combustion is close to $KBO_2$ but closer to $B_2O_3$ in BKN/ACl.

The small amount of magnesium present in the particulate detected in BKN/CsCl and BKN/KCl {see Table 19} most likely originates from the nearly 5% magnesium impurity found in the amorphous boron used in BKN. There is a bias between the total solids collected on the Anderson impactor and the sum of elements and ions collected for the BKN compositions even when oxygen is accounted for accompanying magnesium and $K_xB_yO_z$. It is unknown if the weight differential is due to incomplete recovery of the solids, moisture or hydrogen content in the particulate or the presence of water insoluble/acid insoluble {WIAI} material. Borates are either water or acid soluble. Perhaps there is residual uncombusted boron in the particulate. Elemental boron is difficult to digest with acid.

**Table 21: Calculations for three-gram BKN/MCl tests in a 100 cubic foot chamber**

| Calculation | 22Z | | 22G | | 22M | |
|---|---|---|---|---|---|---|
| | BKN/CsCl | | BKN/KCl | | BKN/ACl | |
| | 24 | 25 | 28 | 29 | 33 | 34 |
| mg/$m^3$ Cs from [Cl] | 101 | 82 | | | | |
| mg/$m^3$ Cs from Analysis | 100 | 78 | | | | |
| mg/$m^3$ K as KCl | | | 25 | 21 | 30 | 25 |
| mg/$m_3$ K in KxByOz | 16 | 12 | 5 | 5 | 2 | 3 |
| K/B mole Ratio | 0.77 | 0.77 | 0.42 | 0.45 | 0.10 | 0.22 |
| mg/$m^3$ MCl | 127 | 100 | 48 | 40 | 57 | 48 |
| mg/$m^3$ KxByOz | 37 | 28 | 17 | 15 | 16 | 17 |

**Table 22: Calculations for three-gram HCE Baseline tests in a 100 cubic foot chamber**

| Calculation | HCE Baseline | |
|---|---|---|
| | 36 | 37 |
| $mg/m^3$ Cl in $ZnCl_2$ | 134 | 134 |
| $mg/m^3$ Cl in CxClyOz | 35 | 35 |
| $mg/m^3$ $ZnCl_2$ | 258 | 258 |
| g $ZnCl_2$ in 100 $ft^3$ chamber | 0.73 | 0.73 |

More molar equivalents of chloride are present in the water soluble component of the particulate produced from HCE baseline combustion than can combine to form $ZnCl_2$ {Table 22}. It is postulated that this chloride originates from water soluble, partially combusted hexachloroethane, $C_xCl_yO_z$. There is a bias between the total solids collected on the Anderson impactor and the sum of elements and ions collected for the HCE baseline obscurant even when oxygen is accounted for accompanying aluminum in $Al_2O_3$ and carbon and oxygen are accounted for accompanying partially oxidized hexachloroethane products postulated as $C_xCl_{2y}O_z$. It is assumed that this is WIAI including $Al_2O_3$, graphite or $C_xCl_yO_z$ components that are acid insoluble. It could also be due to moisture content in the solid that was collected. The literature states that halocarbon vapors are present in HCE baseline combustion products (1).

The amount of zinc chloride detected in the hundred cubic foot tank is 258 $mg/m^3$ {Table 22}. The volume in the 100 cubic foot tank is equivalent to 2.83 cubic meters. Thus, over 0.7 grams of zinc chloride particulate was found in the tank, a quarter of the weight and a 32% yield of the three gram pellet tested therein. This suggests inefficient aerosol formation and/or significant settling of the particulate during the 20 minute test period.

Particulate exposure levels of potential components of the obscurant smokes were identified (21). The ACGIH Eight-Hour Permissible Exposure Level for fumed zinc chloride is 1 $mg/m^3$. The corresponding Short Term Exposure Limit {STEL, 15 minute exposure limit} is 2 $mg/m^3$. The amount detected in the hundred cubic foot tank {Table 22} is 130 times higher than the STEL.

No data are available on PELs for alkali metal chlorides such as potassium chloride or cesium chloride. PELs for alkali metal hydroxides are 2 $mg/m^3$ (Table 23). The low exposure levels for metal hydroxides may be due more to the causticity of the hydroxide. It is expected that the PELs for alkali metal chlorides would be significantly higher. Animal toxicity data suggest that neither the alkali metal hydroxides nor chlorides are extremely toxic (11). Oral rat $LD_{50}$ values are indeed lower for hydroxide salts than chloride salts. Cesium salts have slightly lower oral rat $LD_{50}$ values than the corresponding potassium salts. Zinc chloride has lower $LD_{50}$ values than the alkali metal chlorides. Borate compounds have an ACGIH PEL {8 h time weighted

average} of 21 mg/$m^3$ and a STEL of 61 mg/$m^3$. Boron oxide, $B_2O_3$, has an OSHA PEL of 15 mg/$m^3$. In summary, particulate toxicity of the BKN/halide salt combustion products appears to be less than that of the HCE baseline even if smoke levels increase to produce the same transmittance values.

**Table 23: Comparison of LD50 values for potassium and cesium salts**

| Cation | Chloride Oral Rat $LD_{50}$ | Hydroxide Oral Rat $LD_{50}$ |
|---|---|---|
| Potassium | 2600 mg/kg | 1230 mg/kg |
| Cesium | 1550 mg/kg | 1030 mg/kg |
| Zinc | 350, 1100 mg/kg | |

### 5.3 Divalent Metal Oxidizers with Ammonium Halide Fuels

The baseline HCE obscurant uses hexachloroethane as a halide source to produce zinc chloride from zinc oxide. In the process, toxic halocarbon by-products are produced. One of the distinguishing characteristics of zinc chloride, the primary component in HCEobscurant smoke, is that it is deliquescent, forms hydrates with water and is very water soluble, 4320 g/l at 25 °C. This allows particulate to absorb moisture from the air producing condensed microdroplets, an effective obscurant smoke. Other divalent metal halides are also water soluble and hygroscopic: [$CuCl_2\{H_2O\}_3$] {1104 g/l at 0°C}, [$CaCl_2\{H_2O\}_6$] {5360 g/l at 20 °C}, and [$CaI_2\{H_2O\}_6$], {16800 g/l at 30 °C}. Formulations were developed to produce divalent metal halides using zinc, copper and calcium oxidizers combined with ammonium halides as the halide source. Hydrogen chloride formulation is possible upon combustion of ammonium chloride with these oxidizers but phosgene formation is highly unlikely. Thus, such obscurant candidates should produce smokes that are less toxic than that of the HCE baseline.

#### 5.3.1 Thermochemical Modeling

Thermochemical calculations were conducted on potential HCE smoke replacement formulations containing divalent metal oxidizers and ammonium halide salts {Table 24} in the presence of either an aluminum or elemental boron fuel. These formulations mimic the HCE baseline formulation except that another halide source is present besides hexachloroethane. In many cases, the flame temperatures are as low as those of the HCE baseline. In the case of calcium iodate formulations, ammonium iodide was added to the formulation. This is not necessary as reduction of calcium iodate will form calcium iodide.

In the case of the reaction of zinc oxide with ammonium chloride in the presence of boron, the yield of zinc chloride is predicted to be lower in the combustion products than for the HCE baseline because not all of the zinc oxide is converted to the chloride. Apparently, boron is not as effective as a reducing agent as aluminum. In experimental tests, the HCE baseline was rather difficult to ignite however. Compositions with boron tend to ignite more readily. As more boron is added to the composition, a greater preponderance of boron oxides is formed, however. The boron oxides are predicted to be more efficient as an obscurant than aluminum oxide.

**Table 24: Combustion modeling data for divalent metal oxidizers with ammonium halides**

| HCEsub ID | Oxidizer | Halide Donor | Fuel | NASA-Lewis Equiv. Ratio | Flame Temp. @ 1 atm (K) | Flame Temp. @ 1 atm w/ 2X air (K) | FT-FT w/ 2X air (K) | Mass Fraction at 25 C of 2 parts air to 1 part Composition | | | | | | | | Gas Fraction |
|---|---|---|---|---|---|---|---|---|---|---|---|---|---|---|---|---|
| | | | | | | | | MX2 (S) | MoxO (S) | $M_{ox}(OH)2$ (S) | $M_{fuel}O$ &OH | H2O | HCl (G) | Other | Other | |
| 2519-16A | 46.5% ZnO | 44.5% HCE | 9% Al | 1.50 | 753 | 826 | -73 | 0.256 | 0.002 | 0.000 | 0.057 | 0.000 | 0.000 | CO2 | 0.055 | 0.08 |
| 2519-23P | 53.0% ZnO | 44.5% ACl | 2.5%B | 2.46 | | 1061 | | 0.189 | 0.064 | 0.000 | 0.032 | 0.013 | 0.000 | | | |
| 2519-23Q | 50.5% ZnO | 44.5% ACl | 5.0%B | 2.81 | 442 | 1396 | -954 | 0.209 | 0.047 | 0.000 | 0.061 | 0.012 | 0.000 | | | 0.16 |
| 2519-23R | 48.0% ZnO | 44.5% ACl | 7.5%B | 3.17 | | 1624 | | 0.189 | 0.047 | 0.000 | 0.092 | 0.013 | 0.000 | | | |
| 2519-23W | 50.5% CuO | 44.5% ACl | 5.0%B | 2.16 | 547 | 1348 | -801 | 0.186 | 0.000 | 0.073 | 0.061 | 0.013 | 0.000 | | | 0.34 |
| 2519-23X | 42.0% CuO | 53.0% ACl | 5.0%B | 2.52 | 547 | 1387 | -840 | 0.222 | 0.000 | 0.011 | 0.063 | 0.013 | 0.000 | | | 0.29 |
| 2519-23T | 50.5% BCN | 44.5% ACl | 5.0%B | 1.55 | 769 | 1252 | -483 | 0.186 | 0.000 | 0.002 | 0.061 | 0.013 | 0.000 | Cl2 | 0.0001 | 0.61 |
| 2519-23U | 55.0% BCN | 40.0% ACl | 5.0%B | 1.40 | 1008 | 1218 | -210 | 0.168 | 0.000 | 0.029 | 0.061 | 0.013 | 0.000 | Cl2 | 0.0001 | 0.57 |
| 2519-23V | 55.0% BCN | 42.5% ACl | 2.5%B | 1.27 | 527 | 889 | -362 | 0.178 | 0.000 | 0.020 | 0.031 | 0.014 | 0.000 | Cl2 | 0.0001 | 0.71 |
| 2519-23I | 78.5% CaO2 | 16.5% ACl | 5%B | 1.00 | 2029 | 1226 | 804 | 0.057 | 0.059 | 0.152 | 0.050 | 0.000 | 0.000 | | | 0.43 |
| 2519-23H | 72.5% CaO2 | 25.0% ACl | 2.5%B | 1.00 | 1722 | 1000 | 722 | 0.086 | 0.000 | 0.191 | 0.031 | 0.003 | 0.000 | | | 0.38 |
| 2519-23J | 58.5% CaO2 | 39.0% ACl | 2.5%B | 1.30 | 1358 | 1136 | 221 | 0.135 | 0.000 | 0.111 | 0.031 | 0.054 | 0.000 | | | 0.29 |
| 2519-23K | 47.5% CaO2 | 50.0% ACl | 2.5%B | 1.59 | 1019 | 1241 | -222 | 0.173 | 0.000 | 0.047 | 0.031 | 0.094 | 0.000 | | | 0.31 |
| 2519-23Y | 41.5% CaO2 | 56.0% ACl | 2.5%B | 1.59 | 789 | 1290 | -501 | 0.194 | 0.000 | 0.013 | 0.014 | 0.116 | 0.000 | | | 0.36 |
| 2519-23M | 70.0% Ca(NO3)2 x 4H2O | 27.5% ACl | 2.5%B | 0.88 | 2937 | 1928 | 1009 | 0.095 | 0.000 | 0.010 | 0.031 | 0.124 | 0.000 | | | 0.92 |
| 2519-23N | 62.0% Ca(IO3)2 | 33.0% Al | 5.0%B | 1.01 | 1961 | 1046 | 915 | ? | ? | ? | ? | ? | ? | | | 0.91 |
| 2519-23O | 50.0% Ca(IO3)2 | 45.0% Al | 5.0%B | 1.30 | 1803 | 1222 | 581 | ? | ? | ? | ? | ? | ? | | | 0.89 |
| 2519-23F | 70.0% CaO2 | 25.0% ACl | 5% Al | 1.00 | 1958 | 1994 | -36 | 0.086 | 0.000 | 0.182 | 0.031 | 0.012 | 0.000 | | | 0.42 |
| 2519-23G | 65.0% CaO2 | 30.0% ACl | 5% Al | 1.10 | 1771 | 1115 | 656 | 0.104 | 0.000 | 0.153 | 0.031 | 0.030 | 0.000 | | | 0.39 |
| 2519-23L | 45.0% CaO2 | 50.0% ACl | 5% Al | 1.62 | 1111 | 1307 | -196 | 0.173 | 0.000 | 0.039 | 0.031 | 0.103 | 0.000 | | | 0.30 |

The copper based oxidizers, CuO and {$Cu_2${OH}$_3${$NO_3$} {alias BCN}, behaved in the model similarly to zinc oxide when boron was selected as the auxiliary fuel. Lower yields of the copper{II} chloride were formed relative to the HCE baseline because copper{II} hydroxide is also formed. Again, boron oxides are formed that may act as good obscurants. The thermochemical code predicts the possibility of chlorine formation. No chlorine was observed as a combustion product in the baseline composition, however. The compositions 2519-23X and 2519-23T appear to be the most promising.

For the formulations where calcium peroxide is the oxidizer, the hydroxide competes with chloride for calcium in the combustion products. At least in the formulations that were run through the model, the same weight percentage of calcium chloride was not attained as the weight percentage of zinc chloride in the baseline HCE formulation. Higher boron or aluminum levels increase flame temperature and also the amount of hydrogen chloride that is formed at flame temperature that may not fully react with basic species before reactions are quenched with cool air. As the formulations become more fuel rich by increasing the ratio of ammonium chloride to calcium peroxide, higher mass fractions of calcium chloride are produced in the combustion products. Under fuel rich conditions, higher concentrations of hydrogen chloride may also be formed although they are not predicted in the thermochemical model. Formulations 2519-23L and 2519-23Y look compelling as HCE replacement candidates.

Calcium iodate, is an intriguing candidate as an oxidizer that would produce calcium iodide as a combustion product. Ammonium iodide would not need to be added as an iodide donor although it was added in the formulations in the calculations. If ammonium halide is not added as a fuel, the potential for hydrogen halide formation is less. The model did not allow for prediction of products at ambient temperature. At the time of the writing of this report, zinc iodate was identified as potential donor of zinc iodide {water solubility of 4320 g/l at 18 °C}. Iodates are favored as sources of divalent metal halides over chlorites or chlorates since divalent metal salts of chlorites and chlorates tend not to be thermally stable. For example calcium iodate is thermally stable to 540 °C (11) whereas the chlorite decomposes in cold water. Calcium perchlorate may be deliquescent since it is very soluble in water, 1886 g/l at 25 °C.

### 5.3.2 Ingredient Characterization: Metal Diborides as Fuels in Obscurant Formulations

Additional fuels in addition to boron and aluminum were considered for candidate compositions to replace HCE based obscurants. These included magnesium and aluminum diborides (22). Once a promising obscurant containing aluminum, magnesium or boron as a fuel was identified, the diborides were to be substituted in the obscurant candidate formulation to determine if they improved obscurant performance. Hazard sensitivity for these fuels was obtained {Table 24}. They exhibit ESD sensitivity typical of finely divide metal or metalloid powders. To this point, these diborides have not been incorporated into obscurant formulations.

**Table 25: Hazard sensitivity of aluminum and magnesium diborides**

| Material | STR Number | ABL ESD | Bulk ESD | ABL Friction | ABL Impact | Autoignition {SBAT} |
|---|---|---|---|---|---|---|
| AHOPS Requirements | NA | > 0.075 J | NA | > 40 lbs @ 1 ft/sec | >7 cm | >225 F |
| Aluminum Diboride | 31105 | 0.015 J | No Consumption | >750 lbs @ 8 ft/s | >80 cm | >500 ºF |
| Magnesium Diboride | 31106 | 0.005 J | Partial Consumption | >750 lbs @ 8 ft/s | >80 cm | >500 ºF |

### 5.3.3 **Thermal compatibilities**

Compatibility data were collected for divalent metal oxidizers with ammonium chloride and boron where data were not already available (19). Data are summarized in Table 26. A photo of actual VTS samples for the ACl/CuO system after aging are shown in Figure 23 and related DSC thermograms are shown in Figures 24-26. All ingredient pairs appeared to be compatible by ATK guidelines using the DSC method. ACl/ZnO and ACl/CuO were found to be incompatible by the VTS method {see Section 5.3}. The photo in Figure 23 shows the results of the VTS aging study for ACl/CuO; the stoppers for the ACl/CuO combination actually blew off due to gas build up. It appears that ACl reacts with CuO to produce water vapor, ammonia and the blue copper{II} halide by products at relatively low temperatures. Incompatibility for the ACl/BCN pair was not observed until SBAT tests were conducted on 2519-23T, ACl/BCN/B. The combination is considered incompatible if the autoignition occurs below 225 °F; in this case it occurred at 140 °F.

Apparently an acid/base reaction occurs between the ammonium of the ammonium chloride and the oxide or hydroxide of the divalent metal oxides. Thus, several of the HCE candidates for which theoretical thermochemical data are summarized in Table 24 are not viable due to the aforementioned thermal compatibilities of ammonium chloride with copper or zinc oxidizers.

Compatibility of calcium peroxide with ammonium chloride has not been conducted. This peroxide arrived from the vendor after the other compatibility tests were complete. Zinc iodate was recently identified as a zinc iodide donor in potential HCE obscurant replacements. A vendor source for it has been identified (23).

**Table 26: Thermal compatibility data for divalent metal oxidizers with ammonium chloride and boron.**

| Ingredient A | Ingredient B | DSC onset {°C} | VTS {mL/g} | SBAT |
|---|---|---|---|---|
| ACl | NA | 326 °C | NA | |
| ACl | Al | 317 °C, no new exotherms below 200 °C: compatible by DSC | -0.167 ml/g: compatible by VTS | |
| ACl | boron | 305 °C, no new exotherms below 200 °C: compatible by DSC | -0.202 ml/g: compatible by VTS | |
| ACl | BCN | 305 °C, no new exotherms below 200 °C: compatible by DSC | 0.085 ml/g: compatible by VTS | Exothermic onset at 140 °C, sample combusted |
| ACl | CuO | 293 °C, no new exotherms below 200 °C: compatible by DSC | >>2.0 ml/g {tube stoppers ejected: not compatible} | |
| ACl | ZnO | No new exotherms below 200 °C: compatible by DSC | >>2.0 ml/g {tube stoppers ejected: not compatible} | |
| ZnO | Boron | No visible events from 25-350 °C: compatible by DSC | Not Required | |

**Figure 23: "Aged" VTS tubes containing $NH_4Cl$ {left}; 2-tubes of $NH_4Cl$/Cupric Oxide {center}; Cupric Oxide {right}**

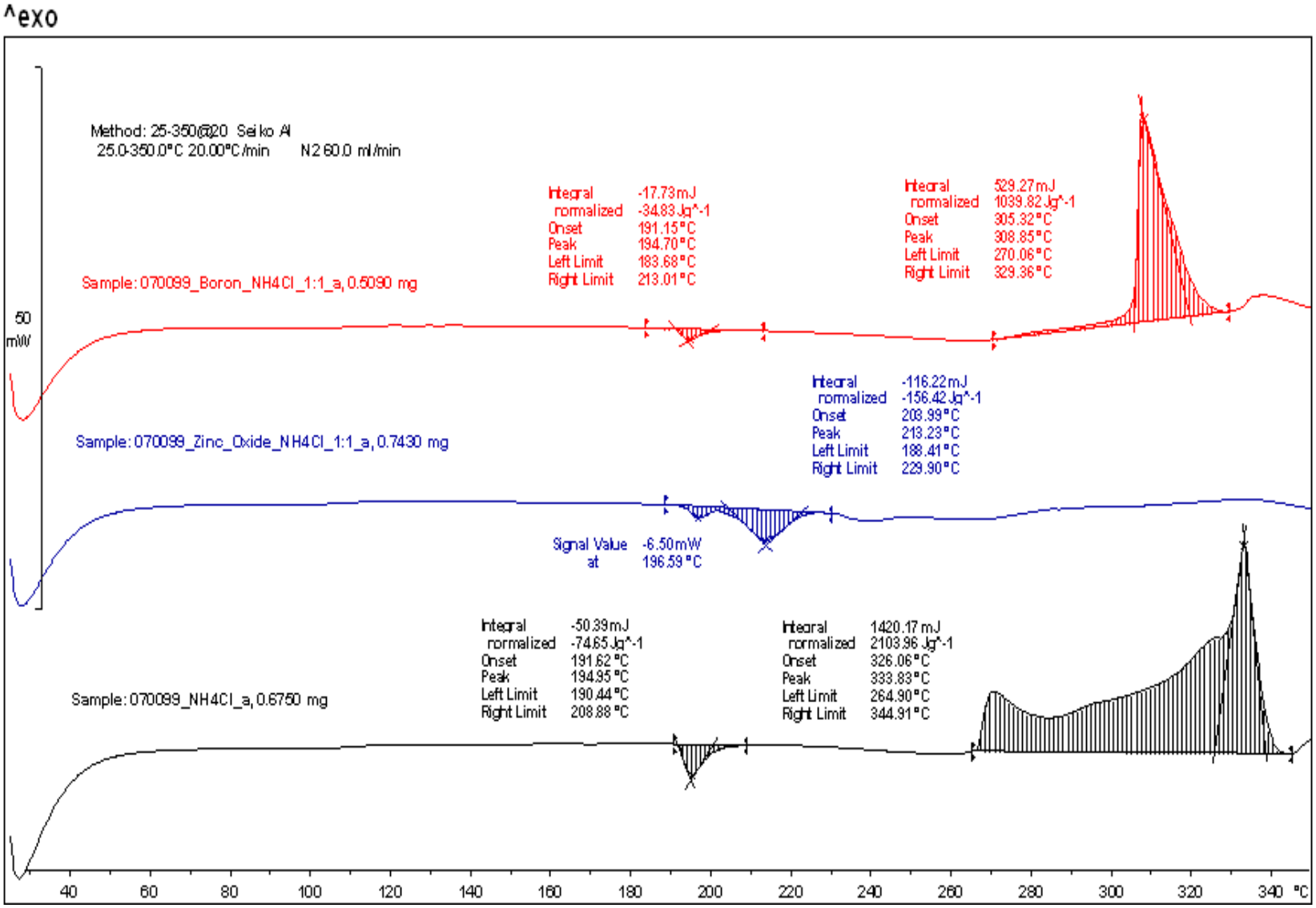


**Figure 24: DSC thermograms for ACl {black}, ACl/ZnO {blue} and ACl/B {red}. The bar along the y-axis is equivalent to 50 mW. Exothermic peaks are positive relative to baseline.**

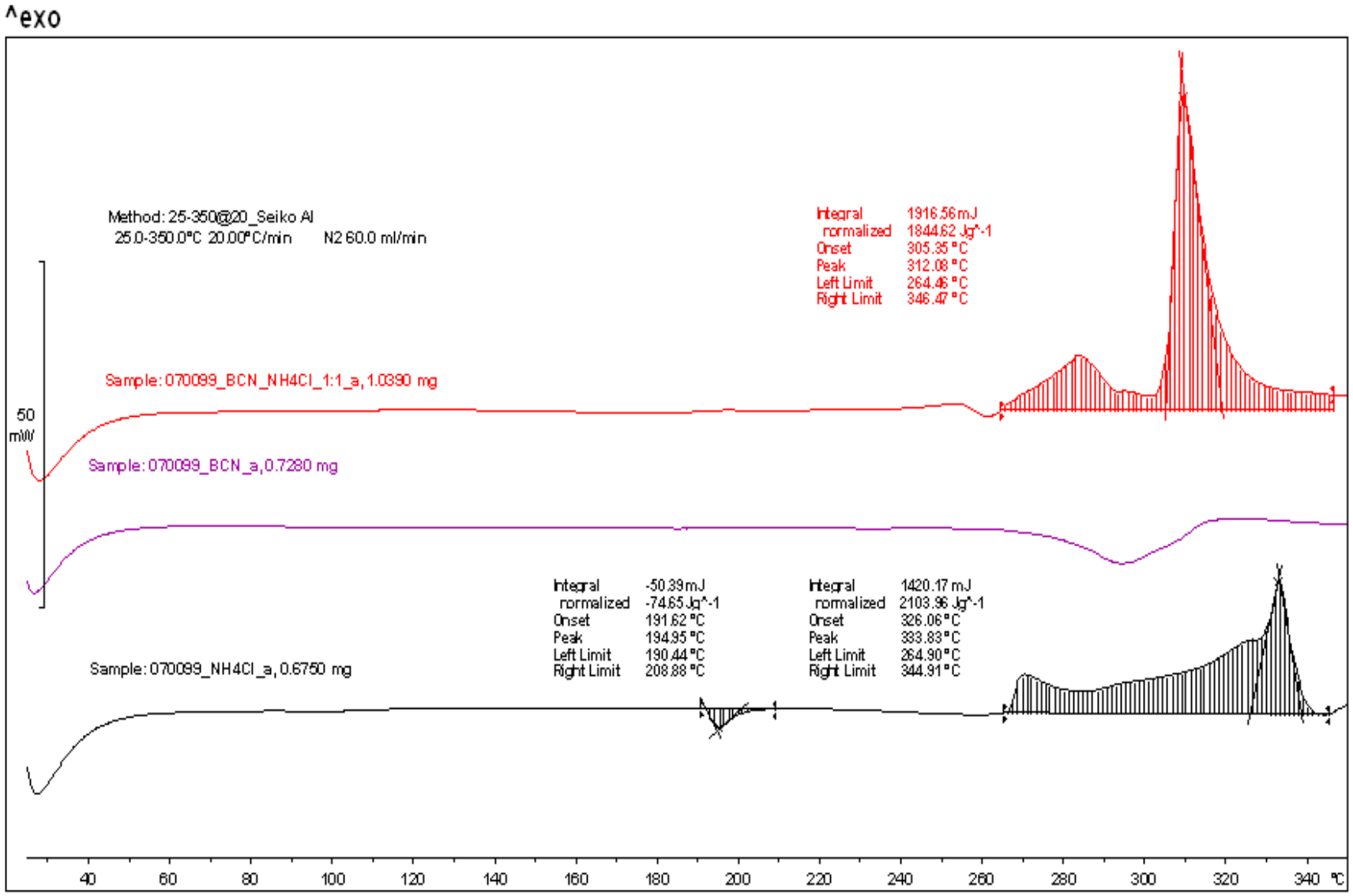


**Figure 25: DSC thermograms for ACl {black}, BCN {violet} and ACl/BCN {red}. The bar along the y-axis is equivalent to 50 mW. Exothermic peaks are positive relative to baseline.**

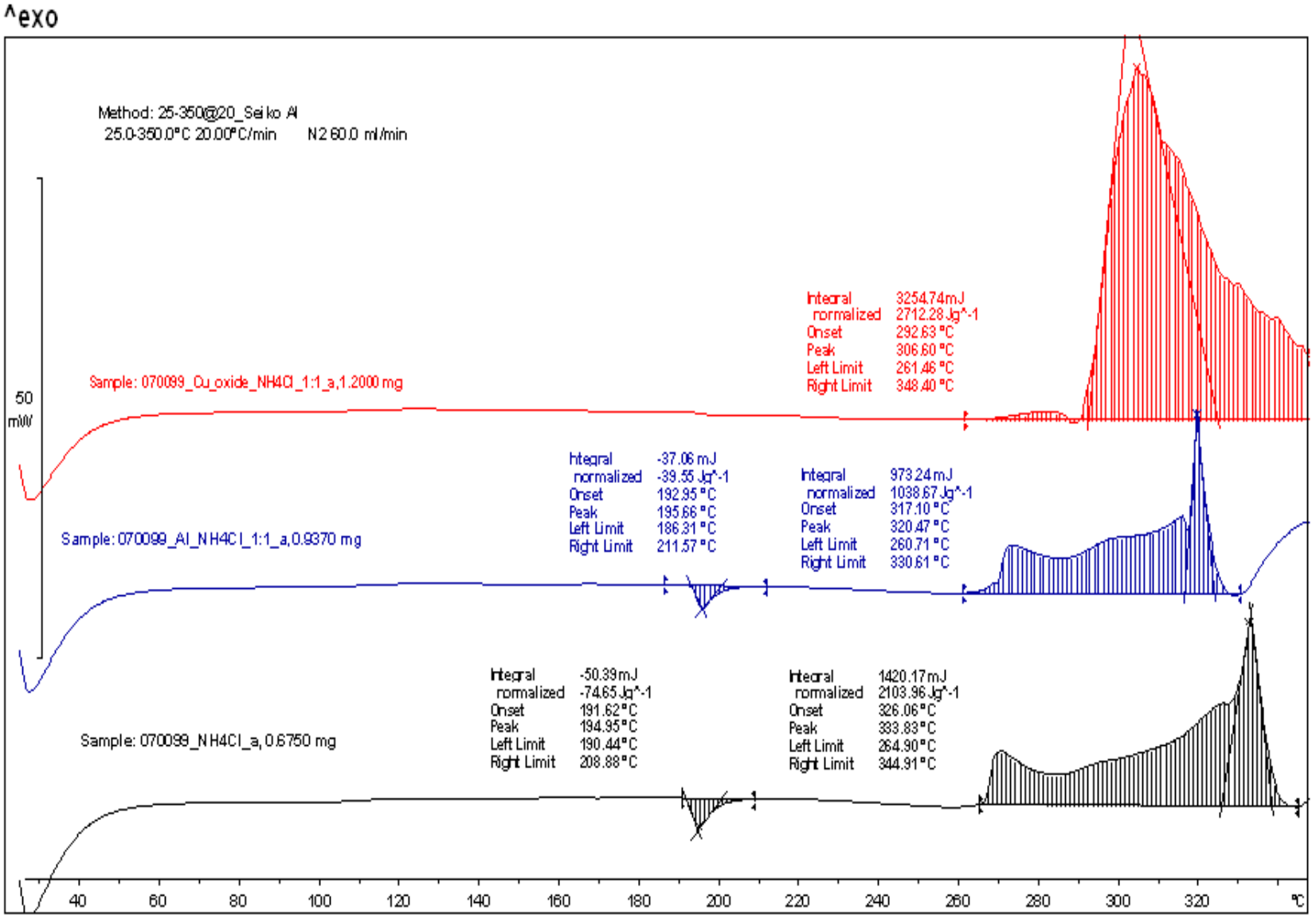


**Figure 26: DSC thermograms for ACl {black}, Al/ACl {blue} and ACl/CuO {red}. The bar along the y-axis is equivalent to 50 mW. Exothermic peaks are positive relative to baseline.**

## 6.0 CONCLUSIONS

Informative, reproducible methods were developed for characterization of the smoke density of particulate aerosols, and the determination of particulate concentrations, particulate particle size distributions as well as the chemical composition of the particles and toxic gases produced from baseline and candidate obscurants. Hazards for processing and testing the obscurants were well defined and controlled.

Compositions containing divalent zinc and copper oxidizers combined with ammonium chloride were deemed to be thermally incompatible. Similar compositions with calcium peroxide, calcium and zinc iodates show promise theoretically.

Compositions containing sodium nitrate, silicon powder and polydimethylsilicone binder improved in performance as the ratio of silicon powder to silicone polymer decreased and the total fuel content increased. Fuel rich formulations that required significant afterburning to complete combustion seemed to produce smoke most efficiently.

Solids produced from the combustion of the specific compositions of boron potassium nitrate igniter blended with halide salts selected for quantitative study were not totally dispersed in aerosol form; significant solid slag formation was observed. The addition of lower levels of the halide salt coolant to the boron potassium nitrate igniter may improve overall obscurant efficiency. This will occur by increasing the flame temperature of combustion allowing for more efficient volatilization of the solid combustion products. Burn rate will increase as coolant levels are decreased in the compositions.

The overall toxicity of combustion gases and particulates is lower relative to the baseline for these formulation families. The baseline hexachloroethane obscurant produced high levels of hydrogen chloride and levels of zinc chloride and phosgene well above OSHA permissible exposure level limits. Formulations with boron potassium nitrate igniter and halide salts produced lower levels of hydrogen chloride, especially the composition containing cesium chloride. No OSHA permissible exposure limits are published for alkali halide particulate. This may suggest that such particulate is of minimum concern by industrial hygienists. No phosgene is produced upon combustion of the blends of boron potassium nitrate igniter with alkali halides although some nitrogen oxide is produced. The oxidizer/fuel balanced ammonium chloride formulation produced measurable levels of nitrogen dioxide also. Of the formulations tested quantitatively, those with cesium chloride were the most efficient candidates on a volumetric basis while producing the lowest level of toxic gases.

## 7.0 RECOMMENDATIONS

Compositions containing boron potassium nitrate igniter blended with halide salts {cesium, potassium and ammonium} were studied in greatest detail during this research effort. Solids produced from the combustion of the specific compositions selected for quantitative study were not totally dispersed in aerosol form; significant solid slag formation was observed. This suggests that a considerable amount of solid combustion products were not converted to smoke and that obscurant efficiency would increase if halide salt were removed from these formulations. This would increase the flame temperature and promote the evolution of more smoke improving obscurant efficiency. Of the formulations tested quantitatively, those with cesium chloride were the most efficient candidates on a volumetric basis while producing the lowest level of toxic gases. It is proposed that further quantitative assessment be conducted on boron potassium nitrate igniter rich compositions containing cesium chloride. Higher levels of

BKN in BKN/CsCl will decrease its packing efficiency. However, if more of the combusted solids form an aerosol instead of slag, transmittance per unit volume of obscurant should still increase significantly.

In initial screening tests, existing candidate obscurant formulations containing boron appeared to produce more smoke than the silicon based candidates. Thus the latter family of formulations was not down selected in the initial SEED phase of this program for quantitative testing in the hundred cubic foot chamber. Compositions containing sodium nitrate, silicon powder and polydimethylsilicone binder improved in performance as the ratio of silicon powder to silicone polymer decreased and the total fuel content increased. Since boron/potassium nitrate formulations appeared to produce more smoke than silicon/sodium nitrate formulations, a comparative quantitative analysis should be conducted to determine the most effective combination using the most promising silicon-based formulation from the current effort as the starting point, e.g.:

1. 10% Si, 30% RTV-615, 60% NaN
2. 10% B, 30% RTV-615, 60% NaN
3. 10% Si, 30% RTV-615, 60% KN
4. 10% B, 30% RTV-615, 60% KN

Once the best combination of fuel and oxidizer has been established, a five point formulation matrix could be tested quantitatively in the 100 cubic foot chambers to further probe performance of the best formulation family as a function of silicone binder content and total overall fuel content with the best formulation from the initial study as one of the corners of the proposed matrix:

5. 10% best fuel, 30% RTV-615, 60% best oxidizer
6. 20% best fuel, 20% RTV-615, 60% best oxidizer
7. 20% best fuel, 30% RTV-615, 50% best oxidizer
8. 20% best fuel, 40% RTV-615, 40% best oxidizer
9. 30% best fuel, 30% RTV-615, 40% best oxidizer

Combustion modeling was conducted on compositions containing divalent metal oxidizers, ammonium halides and a metallic fuel powder, either boron or aluminum. These compositions were predicted to produce significant quantities of deliquescent metal chloride combustion products. Boron combustion products also produce significant quantities of smoke. Compositions containing divalent zinc and copper oxidizers combined with ammonium chloride were deemed to be thermally incompatible. Similar compositions with calcium peroxide also showed promise theoretically. The compatibility of calcium peroxide with ammonium chloride needs to be determined. If compatible, hazard sensitivity data need to be collected on the most promising formulations from the following families, calcium peroxide/ammonium chloride/boron, calcium peroxide/ammonium chloride/magnesium and calcium peroxide/ ammonium chloride/aluminum. This will pave the way for quantitative obscurant and toxicity testing to be completed. Formulations containing calcium and zinc iodates should also follow a similar developmental path. In these latter formulations, the addition of ammonium halide may not be necessary decreasing the chances of hydrogen halide formation. Combustion products from iodate formulations need to be screened for the presence of iodine. Once the best formulation{s} from the calcium peroxide, calcium iodate and zinc iodate families have been

identified, replacement of the metal powder with aluminum diboride or magnesium diboride can be conducted to see if these more novel powdered fuels increase obscurant performance.

## 8.0 REFERENCES


1. **DeVaull GE, Dunn WE, Liljegren JC, Policastro AJ.** *Field Measurement and Model Evaluation Program for Assessment of the Environmental Effects of Military Smokes: Analysis Methods and Results of Hexachloroethane Smoke Dispersion Experiments Conducted as Part of Atterbury-87 Field Studies.* Frederick, MD : US Army Medical Research and Development Command, 1989. AD-A216048.
2. **Cichowicz, J.J.** *Environmental Assessment. Programmatic Life Cycle Environmental Assessment for Smoke/Obscurants. HC Smoke, Vol. 4.* . Edgewood, MD : Chemical Research and Development Center, U.S. Army Armament, Munitions and Chemical Command, U.S. Army Aberdeen Proving Ground, 1983. ARCSL-EA-83007.
3. **Agency for Toxic Substances and Disease Registry.** *Toxicological Profile for Hexachloroethane.* Atlanta, GA : vailable: http://www.atsdr.cdc.gov/toxprofiles/tp97.html, 1997. ATSDR 1997.
4. **Holmes, P.S.** *Pneumomediastinum associated with inhalation of white smoke.* s.l. : Milit Med. 1999;164:751–752.
5. **Katz S, Snelson A, Farlow R, Welker R, Mainer S.** *Physical and Chemical Characterization of Fog Oil Smoke and Hexachloroethane Smoke.* Chicago, IL : IIT Research Institute, 1980. DAMD 17-78-C-8085, AD-A080 936.
6. **H, Cullumbine.** *The toxicity of screening smokes.* s.l. : [PubMed] , J R Army Med Corps. 1957;103:119–122.
7. **Greenfield RA, Brown BR, Hutchins JB, Iandolo JJ, Jackson R, Slater LN, et al.** *Microbiological, biological, and chemical weapons of warfare and terrorism.* . s.l. : [PubMed], Am J Med Sci. 2002;323:326-340. .
8. **Hjortso E, Qvist J, Bud MI, Thomsen JL, Andersen JB, Wiberg-Jorgensen F, et al.** *ARDS after accidental inhalation of zinc chloride smoke.* Intens Care Med. 1988;14:17–24. .
9. **Loh C, Chang Y, Liou S, Jang J, Cheng H, et. al.** *Case Report: Hexachloroethane Smoke Inhalation: A Rare Cause of Severe Hepatic Injuries.* s.l. : Available: http://www.ncbi.nlm.nih.gov/pmc/articles/PMC1459933/.
10. **ASTM International.** *Standard Guide for Assessing the Environmental and Human Health Impacts of New Energetic Compounds.* West Conshohocken, PA : s.n., 2008. E 2552 – 08.
11. **United States National Library of Medicine.** *TOXNET Toxicology Data Network.* Bethesda, MD : http://toxnet.nlm.nih.gov/.
12. **Safety Management Services, Inc.** *ESD Sensitivity Test Equipment.* West Jordan, Utah : http://www.sms-ink.com/products_esd.html, 2011.
13. **Erickson, Chris.** *LWR 40327-ATK Smoke Obscurant Testing.* Ogden, Utah : Autoliv Americas, 2012.
14. **Autoliv Americas.** *LWR 40237 ATK Smoke Obscurant Results.* Ogden, Utah : s.n., 2012.
15. **Hunt-Kramer, Robin.** *LWI-FY12-D0121 DSC and VTS Thermal Compatibility Studies of RTV-615A, RTV-615B, Dow Corning High Vacuum Grease with Sodium Nitrate Grind 218-08-06 and with Silicon 2116 Lot#0042; and Silicon 2116 Lot#0042 with Sodium Nitrate Grind 218-08-06.* Brigham City, Utah : ATK Propulsion Systems, 2011.
16. **ATK Propulsion Systems.** *Hazard Sensitivity Data for Silicone Based Obscurant Candidates.* Brigham City, Utah : s.n., 2011.
17. **Nielson, Daniel.** *Oral recollections regarding obscurant formulations that produce potassium chloride smoke.* Brigham City, Utah : ATK Propulsion Systems, 2010.

18. **Hunt-Kramer, Robin.** *LWI-FY12-D0032 HCE Baseline Thermal Compatibility Tests.* Brigham City, Utah : ATK Propulsion Systems, 2011.
19. —. *LWI-FY12-D0241 Thermal Compatibility Testing of Selected Smoke Ingredient Pairs.* Brigham City, Utah : ATK Aerospace Systems, 2011.
20. **Lesley, Michael W.** *LWI-CY11-0053 Compatibility of Obscurants with D-50 Urethane.* Brigham City, Utah : ATK Propulsion Systems, 2011.
21. **ACGIH.** *Guide to Occupational Exposure Values.* Cincinnati, OH : ACGIH, 2011.
22. **Cutler, Raymond.** *Ceramatec Metal Boride Memo 12-16-2010.* Salt Lake City, Utah : Ceramatec, Inc., 2010.
23. **American Elements.** *http://www.americanelements.com/zniat.html.* Los Angeles, California : s.n., 2012.